Finite Element Analysis of CFRP Prestressed Concrete Beams

By

Debarshi Das

A Thesis submitted to the Faculty of Graduate Studies of

The University of Manitoba

in partial fulfillment of the requirements of the degree of

MASTER OF SCIENCE

Department of Civil Engineering

University of Manitoba

Winnipeg, Manitoba, Canada

ABSTRACT

This thesis investigates the shear capacities of carbon-fiber reinforced polymer (CFRP) prestressed concrete T-beams using a non-linear finite element analysis. The finite element models on ANSYS are validated with the experimental results of four beams having the shear span-to-depth (a/d) ratios of 1.5, 2.5 and 3.5 subjected to four-point bending and that of a beam subjected to a uniformly distributed load. The numerical results are within 10% range of accuracy in comparison to the experimental results. The validated models are used to investigate the influence of the a/d ratios and the prestressing force level on the beam capacity. The analysis indicates that the shear capacity of the beams is inversely dependent on the a/d ratio. It also shows that the increase in the prestressing force by 37% results in a 5.1% increase in the beam shear capacity. The comparison of the analysis results and the North American design shear formulas shows that the formula given by the CSA S806-12 gives similar a/d dependency but lower values of shear resistance than the analysis.

ACKNOWLEDGEMENT

I would like to express my deepest and sincere gratitude to my advisor Dr. Dagmar Svecova, P.Eng, in the Department of Civil Engineering at the University of Manitoba, for her guidance, continuous encouragement and limitless support throughout the course of this research program. I would also like to express equally my sincere thankfulness to my co-advisor Dr. Nipon Rattanawangcharoen PhD, P.Eng, for his valuable advices, efforts and time during the entire research phase.

I would also like to acknowledge the financial support received from the Natural Sciences and Engineering Research Council of Canada (NSERC) towards this research and scholarship awarded from the University of Manitoba.

Finally, I would like to express my deepest reverence to my parents, my wife for their invaluable support throughout the graduate study.

DEBARSHI DAS

TABLE OF CONTENTS

LIST OF TABLES

LIST OF FIGURES

LIST OF SYMBOLS

a = shear span length between point load and the support point (mm)

A_p = area of prestressed tendon (mm^2)

A_v = area of transverse reinforcement (mm2)

A_s = area of non-prestressed longitudinal reinforcement (mm^2)

b = the width of the member where stresses are calculated (mm)

b_w = minimum effective web width (mm)

d = effective depth of reinforcement (mm)

d_s = diameter of a stirrup (mm)

d_v = effective shear depth (mm)

E_{cexp} = experimental modulus of elasticity of concrete (MPa)

E_f = modulus of elasticity of FRP longitudinal reinforcement (MPa)

E_p = modulus of elasticity of prestressing tendon (MPa)

E_s = modulus of elasticity of steel longitudinal reinforcement (MPa)

E_{vFRP} = modulus of elasticity of FRP transverse reinforcement (MPa)

f'_c = compressive strength of concrete determined from tests (MPa)

f_{cr} = cracking or tensile strength of concrete (MPa)

f_{Fu}= ultimate strength of FRP reinforcement

f_{po} = stress in prestressing steel when the stress in the adjacent concrete is zero (MPa)

f_{fb} = specified tensile strength of the straight portion of a bent FRP stirrup (MPa)

f_{pu} = ultimate tensile strength of the prestressing tendon (MPa)

F_{pe} = effective prestressing force in concrete after losses (MPa)

k_m = factor accounting for effect of moment at a section of the member on its shear strength

k_r = factor accounting for longitudinal reinforcement rigidity on member shear strength

M_{dc} = decompression moment equal to moment required to remove initial camber (kN.m)

M_f = factored applied bending moment (kN.m)

N_f = factored applied axial force (kN)

P_{exp} = experimental load capacity of the beams (kN)

r = radius of curvature of the bend of an FRP stirrup (mm)

s = spacing of transverse shear reinforcements (mm)

V_c = concrete contribution to shear strength (kN)

V_f = factored applied shear force (kN)

V_{FRP} = FRP stirrups contribution to shear resistance (kN)

V_r = nominal shear capacity (kN)

V_p = vertical component of the prestressing force (kN)

β = factor accounting for aggregate interlock in concrete sections

ε_x = longitudinal strain at mid-depth of the section

ε_v = Strain in FRP stirrups

ρ_f = longitudinal FRP reinforcement ratio (%)

θ = angle of inclination of principal diagonal compressive stresses with respect to the longitudinal axis (Degrees)

σ_v = stress calculated according to CSA-S6-10 Clause 16.8.7

ϕ_c = resistance factor for concrete

ϕ_{FRP} = resistance factor for FRP

ϕ_{bend} =factor accounting for the reduction in the strength of the FRP stirrup at the bend

ϕ_s = resistance factor for steel reinforcement

ϕ_p = resistance factor for prestressing tendon

LIST OF ABBREVIATIONS

ACI = American Concrete Institute

ASCE=American Society of Civil Engineers

AFRP = Aramid Fiber Reinforced Polymer

CFCC = Carbon Fiber Composite Cables

CFRP = Carbon Fiber Reinforced Polymer

CPCI = Canadian Precast/ Prestressed Concrete Institute

CSA = Canadian Standards Association

FE= Finite Element

FEA= Finite Element Analysis

FRP = Fiber Reinforced Polymer

GFRP = Glass Fiber Reinforced Polymer

HYSD = High Yield Strength Deformed Bar

Chapter 1

INTRODUCTION

1.1. General

Over the past few years, advanced composite materials such as fibre reinforced polymers (FRP) are rapidly used as reinforcement in place of conventional steel in prestressed and non-prestressed concrete structures especially in bridges and parking structures. Understanding their response during loading is crucial for the development of an overall efficient, economic and safe structure.

Of all types of failure noticed in concrete structures, a shear failure is known to be the worst type of failure because the member fails without any prior warning. The research in the area of the shear behaviour of reinforced concrete and prestressed concrete is well-provided but the study on the shear behaviour of FRP prestressed concrete structure is still limited. This is especially true for a concrete T-beam prestressed with FRP tendons. Therefore, in this study, a non-linear finite element analysis (FEA) of concrete T-beams prestressed with carbon fibre reinforced polymer prestressing strands (CFCC) is conducted to investigate their shear behavior. Here two main parameters: the shear span-to-depth (a/d) ratio and the level of the prestressing force; are considered. To achieve this, the finite element (FE) models in ANSYS are first constructed and validated against the experimental work conducted by Nabipaylashgari (2012) at the University of Manitoba. The construction of the FE models and the validation of the results are presented in chapter 3 and chapter 4, respectively. Using the model, the parametric study is carried out and the results are compared with the shear capacities calculated from the North American codes. The discussion of the results is presented in Chapter 4.

1.2. Objective and Scope

The scope of the project includes a non-linear FE investigation of six prestressed T-beams without web reinforcement subjected to four-point bending with different a/d ratios ranging from 1.5 to 4.0 and a prestressed beam subjected to a uniformly distributed load. Only two parameters are considered, i.e. the a/d ratio and the level of the prestressing. Other parameters such as material strengths and properties; member dimensions; size and number of the CFCC and of the FRP reinforcement; and the configuration and the number of the CFCC tendons are not varied.

The objectives of this research are to:

- Construct and validate the FE models of the CFCC prestressed T-beams subjected to four-point bending with different a/d ratios and of a beam subjected to uniformly distributed load;
- Conduct parametric study to investigate the effect of a/d ratios and the level of prestressing forces on the shear behavior of the beams.
- Evaluate the adequacy of the current shear design formulas in Canadian and the United States design codes and guidelines for FRP prestressed concrete beams.

1.3. Research Significance

In the past few decades, FEA have been widely used for the analysis of steel reinforced and steel prestressed concrete beams. However, there is a limitation on the availability of the research on the analysis of an FRP prestressed beam. The thesis mainly aims to study the dependency of the CFCC prestressed beam shear capacity on the a/d ratio and the level of the prestressing force. The results of the study may provide a mean to review the shear formula in the current codes specifically for the CFCC prestressed T-beams.

1.4. Thesis Organization

This thesis consists of five chapters. The contents of each chapter are as follows:

- Chapter one presents an introduction to the study, the research objectives and the scope of the work.
- Chapter two consists of literature review on the application of the FE techniques to non-prestressed and prestressed concrete beams.
- Chapter three provides the detail procedure for the construction of the FE models of the beams under consideration in ANSYS.
- Chapter four presents the analysis and the verification of the results. It also includes the parametric study, the discussion and the evaluation of the North American codes in terms of shear capacity.
- Chapter five summarizes the conclusions from the study and presents the recommendations for future work.

Chapter 2

LITERATURE REVIEW

2.1. General

FEA is a unique tool to perform non-linear analysis of reinforced concrete beams to study various responses when subjected to external loads. In this chapter, the wide applications of FEA used by previous researchers to study different behavioral aspects of reinforced concrete beams are discussed. Section 2.2 discusses the use of FEA to predict the flexural behavior of prestressed concrete beams. Section 2.3 and 2.4 present the capacity of FEA to simulate the shear behavior of the non-prestressed and of the prestressed beams, respectively.

2.2. FEA of FRP Prestressed Beams

T.H.Kim (2010) used ANSYS to study the non-linear flexural responses of rectangular concrete beams prestressed with two AFRP tendons. Two tested beams were selected for the simulation purpose (McKay 1992, Sen et al. 1999). The beams were simply supported and tested under four point bending. The prestressing level for the first beam and for the second beam was 60% and 55% of the ultimate strength of the AFRP tendon, respectively. The comparisons between the ANSYS results and experimental results were made in terms of flexural responses. The numerical models accurately predicted the experimental response with a maximum error of less than 5% at ultimate.

Wang et al. (2011) also carried out a non-linear analysis of the concrete beams prestressed with FRP tendons to study the behavior in flexure using ANSYS. The authors conducted tests on eight prestressed rectangular beams and the test results were used for the non-linear analysis. The results from FEA were within 5% of the test results in terms of the ultimate load and the load-

deflection responses. The FE models were further used to investigate the influence of the prestressing force and concrete strength on the behavior of the beams.

A recent research demonstrated the capability of the FEA in simulating the flexural behavior of T-shaped girders prestressed with CFCC (Grace et al. 2013). The span and width of T-beams were 9.45 m and 2.59 m, respectively. The beams were prestressed with 7-15.2 mm diameter CFCC and the prestressing level was 60% of the ultimate. The beams were tested under simply supported condition and subjected to concentrated load at mid span. The analytical model for the beams was developed using commercial software ABAQUS. The FE results showed good correlations with the test results in terms of the ultimate load, the failure mode and the load-deflection responses.

2.3. Shear Study of Non-Prestressed Concrete Beams by FEA

Dirar et al. (2005) carried a FEA on two span continuous deep concrete beams. The geometry and the internal reinforcement were the same for all the beams considered. Three different types of deep beams were studied in the experiment based on concrete strength and the web reinforcement ratio. The beam cross-section was 90×625 mm. The beams were loaded in four point bending to failure. The commercial FE package DIANA was used in the analysis. Shear retention was the only parameter varied in the analysis. The predicted results by DIANA were in good agreement with the experimental results and the failure load estimation was within 5%. The beams failed in shear during the test and the same mode of failure was identified by the FE models.

Similar study was carried out in three Japanese organizations of Public Works Research Institute and Kyushu Institute of Technology in collaboration with Hanshin Expressway Public Corporation (Unjoy et al. 2004). The objective of the research was to investigate the failure load,

the failure mode, and the crack propagation of RC underground deep beams subjected to vertical and lateral loads. A total of nineteen beams were tested under two concentrated loads. The spans of these beams were kept constant but the longitudinal-to-vertical reinforcement ratio, the shear span, the cross section, and the yield strength of the longitudinal reinforcement were varied. The beams had the shear span-to-depth ratio, a/d ratio, between 0.5 and 1.5, the effective depth ranged from 400 mm to 1400 mm and the lateral reinforcement ratio of 0%, 0.4% and 0.8% within the shear span. The analytical simulation of these beams was conducted by Salamy et al. (2005) using DIANA. The study showed that the FE model predicted the load-deflection response, the ultimate load and the crack pattern closely to those observed in the experiments and with acceptable range of accuracy. However, the analytical model overestimated the failure load by 20% for the beams with the a/d ratio of less than unity because of rigid bond assumption between concrete and steel reinforcement.

Kamonna (2010) used ANSYS to carry out a non-linear analysis of his experiments on twelve simply-supported deep beams subjected to a single concentrated load at mid span. All the beams had the same span (600 mm) and the same width (75mm) and were divided into three groups based on the reinforcement ratio and the presence or the absence of the steel fibers in concrete. The overall depth of the beams in each group was 400 mm, 300 mm, 200 mm and 150 mm resulting in span-to-depth ratios of these beams to be 1.5, 2.0, 3.0 and 4.0, respectively. In the FE models, two different techniques were employed to represent the steel fibers in concrete. In the first approach, the mechanical properties of concrete were enhanced to encompass the presence of steel fibers. The second approach assumed the steel fibers to be smeared in concrete element. The results of the FEA showed close simulation of the experimental results. It was found that the smear model provided better response in terms of the accuracy.

Saifullah et al. (2011) carried out a non-linear analysis of rectangular reinforced concrete beams for different patterns of shear reinforcements using ANSYS. The objective of the research was to investigate the influence of RC beams with and without shear reinforcements on the shear capacity. Six simply supported beams were modeled with and without web reinforcement. The difference in the shear reinforcement pattern was implemented by providing close or open stirrups with different end anchorage conditions (vertical bend, horizontal bend or inclined bend). The experimental data from Backouse (1997) was used to calibrate the FE model. The model correctly predicted the results obtained from that experiment. Similar models were developed to include different shear reinforcement patterns for the other beams. The cracking load, the ultimate load, and the stress in the reinforcement from the FEA were compared with hand calculation as a second verification. The ANSYS results were very close to those of the theoretical calculation. From the FE results, the authors concluded that all types of web reinforcements were effective for the static load condition.

A similar study was conducted to evaluate the shear resistance of high strength rectangular concrete beams without web reinforcement (Reddy et al. 2011). The authors tested eight simply supported beams subjected to four point bending. The specimens were divided into four groups of different a/d ratios of 1, 2, 3 and 4. The cross section and the internal reinforcements of all of the beams were kept identical. The width and depth of the beams were 100 mm and 150 mm, respectively. The beams were made of high strength concrete with compressive strength of 70 MPa and were reinforced with 3-16 mm diameter High Yield Strength Deformed (HYSD) bars to ensure shear failure. All the beams in each group were modeled in ANSYS software and the FE results accurately predicted the diagonal tension failure and the shear compression failure as observed in the tests. The authors proposed a simplified equation to predict the shear capacity

high strength concrete beams without transverse reinforcement using previous database and the ANSYS results.

A FEA of reinforced concrete simply supported deep beams subjected to two point loads (50 KN each) was carried out by Niranjan et al. (2012) to study the behavior in flexure and in shear. Three different spans of the beams were considered for the analysis to provide span-to-depth ratios of 1.25, 1.375 and 1.5. The beam cross-section was kept constant to be 150×400 mm. The analysis was carried out in 2D using 2D plane stress elements. The variation of the flexural stresses and the strain at mid-section and the shear stresses near the supports were found to be close to the values calculated using the Euler-Bernoulli theory. The authors concluded that 2D FEA was sufficient to use in the study of the behavior of rectangular deep beams.

A FE simulation of the shear capacity of GFRP-reinforced concrete beams was performed recently by Abed et al. (2013) using ABAQUS. The authors used the experiments results of five GFRP reinforced concrete beams conducted by Abed et al. (2012) to validate the FE models. In that experimental study, five simply supported beams subjected to four point bending were tested. The span, the width, and the depth of all the tested beams were 2000 mm, 200 mm and 300 mm respectively. The only variables in the beams were the reinforcement ratio and the a/d ratio. Three different a/d ratios were considered (1.08, 1.32 and 1.52) by varying distance between the two point loads. Numerical models of all the five beams considered rigid bond condition between concrete and the reinforcement. Good correlations were observed between the analytical models and the experimental results, mainly in terms of ultimate load and the mode of failure. The mid span deflection and failure load predicted by the ABAQUS models were within 10% range of accuracy. The beams failed in shear during the experiments and the same was confirmed by the numerical study. The research concluded that the FE technique was efficient to

properly model the non-linear behavior of reinforced concrete beams in shear and the verified FE models could be used for further study.

2.4. Shear Study of Prestressed Concrete Beams by FEA

FE formulation based on a secant modulus approach was implemented to study the shear behavior of partially prestressed concrete T-beams with steel fibers (Paramasivam et al. 2005). The authors conducted experiments on eight simply supported beams subjected to a symmetrical two point loading. All beams had identical cross section for both prestressed and non-prestressed reinforcement. The spans were different due to different length consideration in the constant moment zone region which resulted in three types of span-to-depth ratios: 2.00, 2.5, and 3.0. Seven 9.5 mm wire steel strands were used for the prestressed beams while five 16 mm mild steels were used for the non-prestressed beams. The partial prestressing ratio and the volume fraction of steel fibers were varied from 25% to 100% and 0% to 1.0%, respectively. In the FE formulation, developed by the authors, the reinforcement was assumed to be elastic-perfectly plastic and the steel fiber concrete was considered as an orthotropic, non-linear elastic material with stress-strain relations in two principal directions. A smear rotating crack model with four-node quadrilateral element was used. The applied load-deformation, the strain in steel, and the shear strain were well predicted by the FEA. The ultimate loads obtained by the FE formulation were within 15% range of accuracy. However, the load-deflection responses were 15% stiffer than the experimental responses.

A similar work was carried out using ANSYS to study eleven shear critical partially prestressed concrete T-beams with steel fibers over partial or full depth (Ramaswamy et al. 2006). The variables considered in the experiments were concrete compressive strength (35MPa, 65MPa and 85MPa), the a/d ratios (2.65 and 1.59), the presence or the absence of the steel fibers (1.5% and

0%) in the flange, the web or the entire cross section. All the beams were simply supported, had the same cross section and were subjected to two point loading. Only half of the beams were modeled and a bond-slip relationship between concrete and the reinforcement was taken into consideration to simulate the test results. The load predicted by the FE models in various stages of loadings was in good agreement with the test results. The FE model also correctly evaluated the diagonal shear failure and the shear compression. However, the load-deflection curve in the post-cracking region obtained from the tests was stiffer when compared to the FE results. The authors concluded that the discrepancy was due to the variation in the bond-slip model of the reinforcement used in the analysis when compared with that present in the test.

A Non-linear FEA program RCAHEST (Reinforced Concrete Analysis in Higher Evaluation System Technology), developed by Kim et al. (2001) was used to study concrete deep beams with and without prestress (Kim et al. 2011). The experimental results from the work done by Smith et al. (1982) and Tan et al. (1992) were used for verification purpose of the non prestressed and the prestressed concrete beams, respectively. Four non-prestressed simply supported beams subjected to two concentrated load as well as four prestressed simply supported beams subjected to a single mid-span load were simulated in the analysis. The beams in each group were all with the same cross-section and had the same reinforcement configuration. The span lengths were varied. Very good correlation between the test results and the FE results were obtained. The shear mode of failure was predicted accurately by the program and the failure load estimated by FE model was within 6% of the test results.

A similar non-linear analysis of a concrete deep beam prestressed with high tensile steel wires was studied by Kasat et al. (2012). The beam was simply supported and was subjected to a uniformly distributed load. The FE model was constructed in ANSYS and the results from the analysis were compared only with a hand calculation using strut and tie model since no

experiment was conducted. Based on the comparison, ANSYS can predict the behavior of the prestressed deep beam very closely.

Celal (2011) conducted the experiments on the precast/prestressed hollow-core (PHC) slabs subjected to a concentrated load to study the shear behavior of the slabs. The concentrated load was placed at a distance 2.5d or 600 mm, whichever is greater from the left support to ensure shear failure. The length of the bearing, the void shape and size, and the a/d ratio were considered to be variables. A total of twelve PHC slabs were tested. The slabs were subdivided into three groups, four specimens in each group, based on thickness of the slabs. Seven-wire low relaxation steel strands were used as the prestressing reinforcement. The prestressing level was kept the same for all the specimens and was equal to 60% of the rapture stress of the strands. ANSYS was used in the analysis. The FE models were verified against all the experimental results and they were found to provide a reasonable accuracy (8%) in the simulation of the slab behavior. The validated models were used to study the effects of the a/d ratios and the prestressing forces on the shear capacity of the beams.

From the above literature review, it can be seen that FEA is capable to analyze RC beams with and without prestressing effects. Note that shear failure is known to be worst type of failure because it is a sudden failure. The FE technique can correctly predict the shear failure of concrete beams with reasonable degree of accuracy. It is also noticed that ANSYS was widely used in the study of shear behavior of concrete beams. There is, however, limited number of studies available on the analysis of the FRP prestressed beams and there is no numerical investigation reported on the shear behavior of concrete beams prestressed with CFCC which is of interest here. Hence, ANSYS will be used to perform non-linear analyses of the prestressed concrete T-beams in this study.

Chapter 3

FINITE ELEMENT MODELING

3.1. General

Finite element modeling (FEM) is an effective tool to perform nonlinear analysis of any complex structure. FEM considers both geometrical and material nonlinearity and it can be used to solve almost any kind of physical problems encountered in real world. It is also observed during the literature review that this technique enabled researchers (Yang 1994; Wolanski 2004; Celal 2011) to predict nonlinear behavior of reinforced concrete structure with high degree of accuracy. The finite element software package, ANSYS 14, is used to study the shear behavior of concrete T-beams prestressed with CFCC. Total of four categories of beam are considered in this research and the test data is taken from the experiment conducted by Nabipaylashgari 2012 at the University of Manitoba. The outline of the tested beams is shown in Table (3.1).

Table (3.1): Descriptions of Tested Beams considered in this research (Nabipaylashgari 2012)

Beam ID	Number of Samples Tested	Shear Span to Depth Ratio (a/d)	Type of Loading
PR-3.5	2	3.5	Two Point Loads
PR-2.5	2	2.5	Two Point Loads
PR-1.5	2	1.5	Two Point Loads
PR-U	2	-	Uniform Load

In this chapter, all necessary steps to develop the FE model are described in details. This includes the element types, material properties used to properly model concrete, reinforcement, reinforce-concrete interface and steel plates at support and loading location. The mesh size, boundary conditions, and solution control are also explained. The developed models are verified against the test results. The details about the geometry and material properties of the tested beams and the FE model verification are depicted in the next chapter.

3.2. Element Types and Material Properties

3.2.1. Concrete

SOLID65 element type is used to model the concrete as it is used by many researchers to model reinforced concrete beam (Wolanski 2004, Celal 2011, Mostafa 2011) .This is the only element type available in ANSYS 14 to simulate concrete nonlinear material behavior because of its ability of cracking in tension and crushing in compression. This solid element has eight nodes with three translation degrees of freedom in the nodal x, y, and z directions at each node. The element is capable of plastic deformation, creep, cracking in three orthogonal directions, and crushing. The geometry and node definitions for this element are shown in Figure (3.1).When the principle stress exceeds the tensile strength of concrete, the crack starts to develop in the direction perpendicular to the direction of that principle stress.

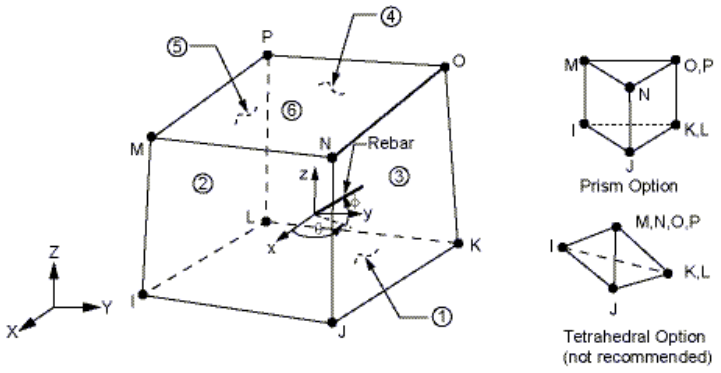

Figure (3.1): SOLID65 ELEMENT (ANSYS 14, 2013)

The SOLID65 element requires linear isotropic and multi-linear isotropic material properties in order to properly model concrete. The multi-linear isotropic material uses the Von-Mises failure criteria along with the William and Warnke (1974) model to define the failure of concrete (ANSYS, Release 14, 2013). In addition, there are other parameters to be set to define the

William and Warnke model. The following subsection will discuss in details of the material modeling of concrete.

a) Linear Isotropic Properties:

Modulus of elasticity (E_c) and Poison's ratio are to be specified for the concrete material. Poisson's ratio is input as 0.2 for the beams considered in this research. However, the experimental values of E_c are specified for specific beams with different a/d ratio under consideration and that can be found in the next chapter.

b) Non-linear Material Properties

The compressive stress-strain curve for concrete has to be specified. A typical stress-strain curve for concrete consists of two parts: an ascending branch and a descending branch. However, the use of the descending branch in ANSYS leads to a convergence problem as encountered by many researchers (Kachlakev et al.2001, Wolanski 2004), hence only the ascending branch of stress-strain curve is considered.

The points on the ascending branch of the compressive multi-linear isotropic stress strain curve are computed based on the following equations (MacGregor 1992).

$$f = \frac{E_c\,\varepsilon}{1+\left[\frac{\varepsilon}{\varepsilon_0}\right]^2} \tag{3.1}$$

$$\varepsilon_0 = \frac{2f_c'}{E_c} \tag{3.2}$$

where:

f= stress at any strain ε, MPa;

ε = strain at any stress f;

ε_0= peak strain at the ultimate compressive strength f'_c

The stress-strain curve shown in Figure (3.2) is for the PR-3.5 beams and the compressive strength of concrete f'_c is equal to 48 MPa. The modulus of elasticity E_c is considered as 28888 MPa as per the test results.

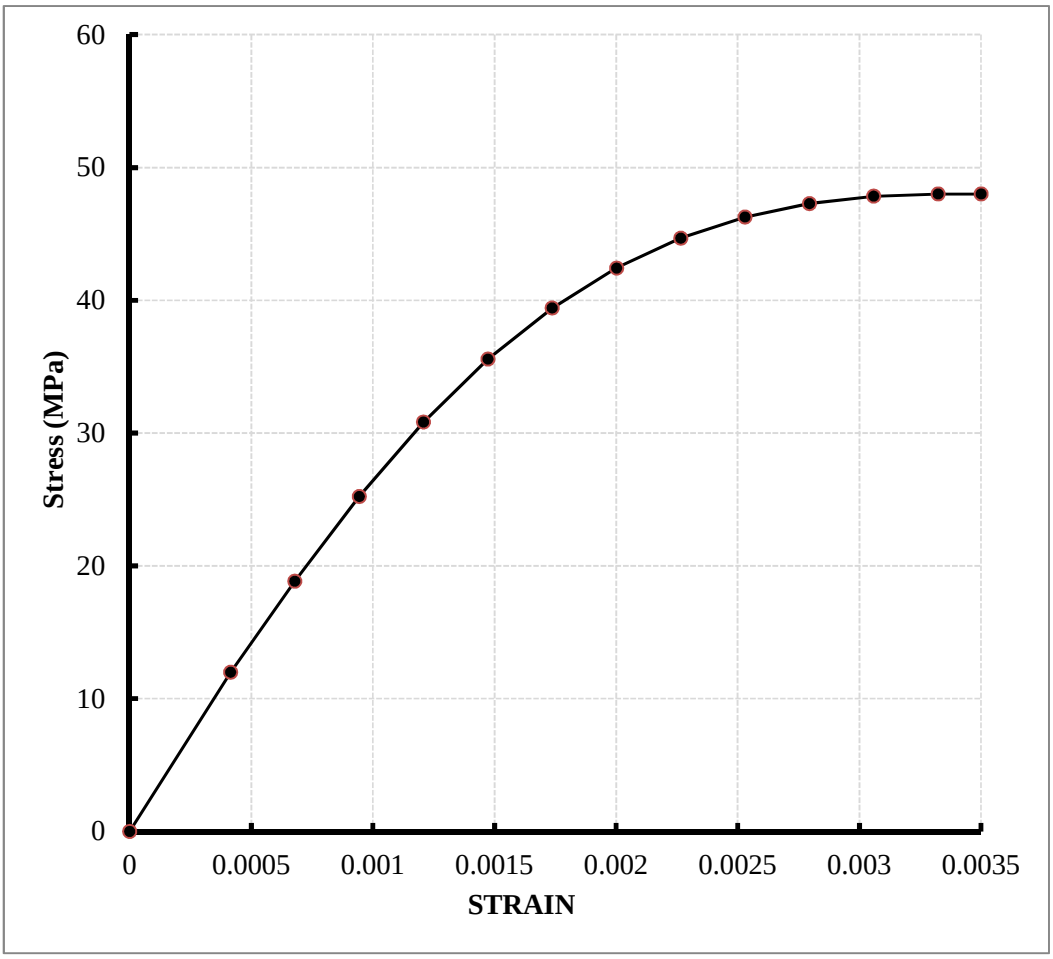

Figure (3.2): Concrete Stress-Strain Curve for PR-3.5 Beams

The first point on the curve must be within the elastic range satisfying Hooke's Law.

$$E = \frac{\sigma}{\varepsilon} \tag{3.3}$$

The first point is calculated based on equation (3.3) corresponding to stress *f* equal to 25% of f'_c. The other intermediate points on the curve are defined based on equation (3.1) and (3.2). The last point is selected at the ultimate compressive strength f'_c and strain equals to 0.0035 which is the traditional crushing strain for unconfined concrete as specified in the CSA A23.3-04 (Canadian Standard Associations, 2004). The stress-strain curves for all the other beams considered in this study are developed in the similar way as explained above and are presented in the Appendix.

c) The tensile strength of concrete is required to input in ANSYS separately hence it is not shown in the concrete stress-strain curve. The following section describes additional parameters to be input in ANSYS and the third parameter refers to the tensile strength of concrete. Additional Parameters

The following nine constants are required to specify in ANSYS in order to implement the William and Warnke material model.

1. Shear transfer coefficient for an open crack (C1);
2. Shear transfer coefficient for a closed crack (C2);
3. Uniaxial tensile cracking stress (C3);
4. Uniaxial crushing stress (C4);
5. Biaxial crushing state (C5);
6. Ambient hydrostatic stress state (C6);
7. Biaxial crushing stress under the ambient hydrostatic stress state (C7);

8. Uniaxial crushing stress under the ambient hydrostatic stress state (C8);
9. Stiffness multiplier for cracked tensile condition (C9);

Typical shear transfer coefficients range from 0.0 to 1.0, with 0.0 representing a smooth crack (complete loss of shear transfer) and 1.0 representing a rough crack (no loss of shear transfer). Convergence problem is encountered when the shear transfer coefficient drops below 0.2 (Kachlakev, et al. 2001). In this research, open (C1) and closed (C2) shear transfer coefficient are considered as 0.3 and 0.95, respectively based on previous studies (Kachlakev, et al. 2001; Wolanski 2004; Celal 2011). The constant C3 is the modulus of rapture of concrete and the values from the test results will be used in this study and are reported in the next chapter. The constant C4 is the ultimate compressive strength of concrete f'_c. Stress concentration under the loading plate and at the support location leads to convergence problem hence the constant C4 is entered as -1 to turn off the crushing capability of concrete element as suggested by past researchers (Kachlakev, et al. 2001; Wolanski 2004). The William and Warnke failure surface can be defined by C3 and C4 (ANSYS 14), the rest of the parameters are left to the default values.

3.2.2. Reinforcement

CFCC is used as prestressing strand and glass fiber-reinforced polymer (GFRP) is used as flange reinforcement for the beams considered in this study. The details of the beams are described in the next chapter. LINK180 is used for all reinforcement here. LINK180 is a 3-D element which can be used to model trusses, sagging cables, links, springs etc. It requires two nodes to model the element and each node has three translational degrees of freedom in the nodal x, y, and z directions (ANSYS 14, 2013). This element is capable of resisting tensile and compressive force

but it cannot sustain any moment. It also supports plasticity, creep, rotation, large deflection, and large strain. Its most important feature used in this study is the ability to have initial strain. The geometry and node locations for LINK180 element used to model the CFCC and GFRP are shown in Figure (3.3).

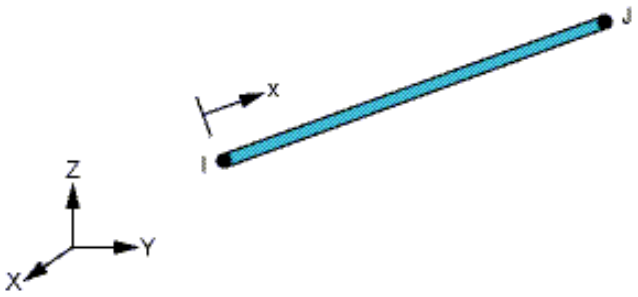

Figure (3.3): LINK180 ELEMENT (ANSYS 14, 2013)

In the present study, a discrete model as shown in Figure (3.4) is used to model the reinforcement.

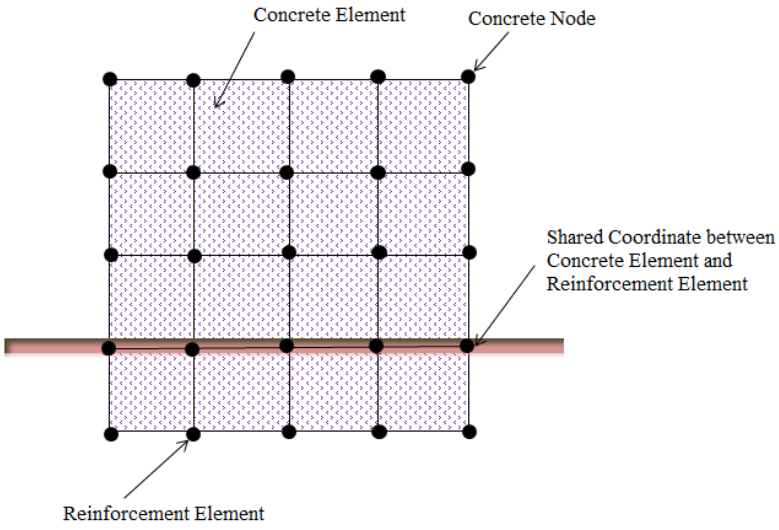

Figure (3.4): Discrete Reinforcement Modeling in Concrete Element

(Reproduced from Tavarez 2001):

The diameter of CFCC and GFRP used for all beams in this research are 12.5 mm and 6 mm, respectively corresponding to the cross sectional areas of 76 mm^2 and 31.67 mm^2. LINK180 element requires a linear isotropic material property and a stress –strain curve to properly model the reinforcement. Since, the CFCC is initially stressed, the initial strain is specified to simulate the prestressed. The following paragraph explains the material modeling for the reinforcement.

a) Linear Isotropic Properties

The modulus of elasticity (E_p) is specified for the CFCC strands and the flange reinforcement (GFRP) using the test results (Nabipaylashgari 2012) as shown below in Table (3.2). Poisson's ratio is input as 0.3 for all the reinforcements.

Table (3.2): Linear Isotropic Properties for Reinforcement

Description	E_p (MPa)
CFCC	136000
GRFP	40800

b) Stress-strain curve for CFCC strand

The stress-strain curves are also needed to define the rapture failure of the CFCC and GFRP reinforcements. The rapture stress for CFCC and GFRP used in this study are 2047 MPa and 827 MPa, respectively based on the tests by Nabipaylashgari 2012. The ultimate strain is calculated by dividing the rapture stress by respective modulus of elasticity. The stress-strain relationships for CFCC and GFRP are linear and are shown in Figure (3.5).

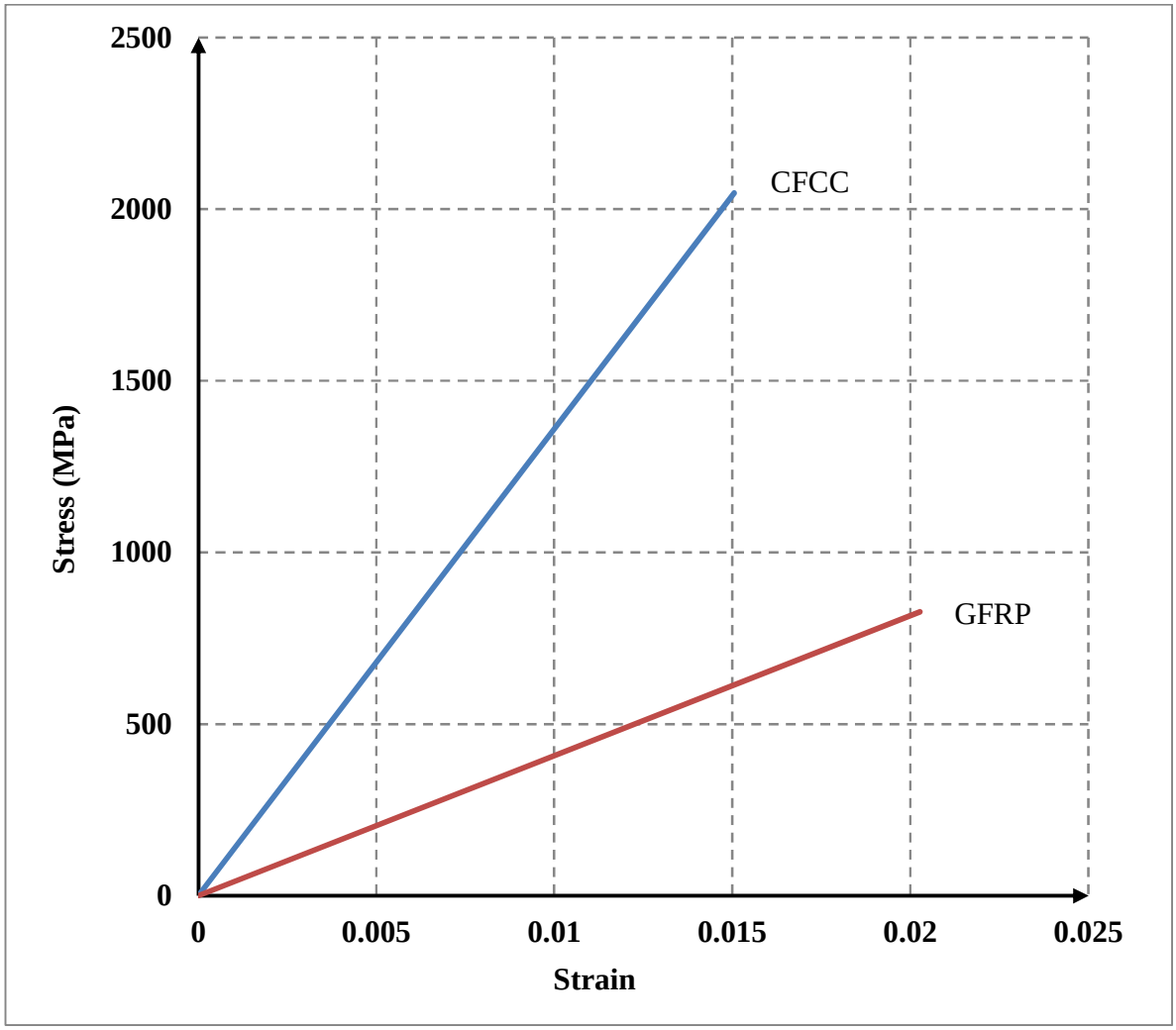

Figure (3.5): Stress-strain curve for CFCC and GFRP

c) Initial Strain

As discussed, LINK180 element has a special feature of initial state condition. Initial stress, strain, temperature etc. can be assigned to this element by INISTATE command. In this study, the initial strain is specified to the prestressing strands in the longitudinal direction to simulate the prestressing force. The beams considered in this project (Table 3.1) had different degree of prestressing force so the specified initial strain is calculated from the corresponding prestress level and the values are shown in the next chapter. The initial strain is transferred to the surrounding concrete at the end of first load step which produced camber along the length of the

beam. The camber for the PR-3.5 beams is shown in Figure (3.6) and the same for other beams are reported in the Appendix.

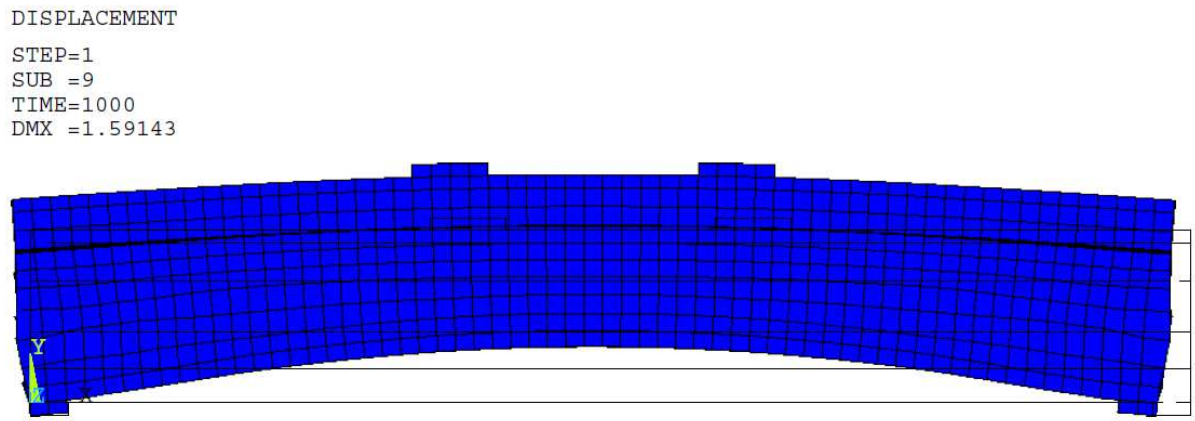

Figure (3.6): Camber for PR-3.5 beams

3.2.3. Steel Bearing Plate

Steel plates are modeled at supports and loading location to avoid stress concentration and local crushing of concrete element which can lead to convergence problem. SOLID185 is chosen to model the steel plates. The element has eight nodes and each node has three translational degrees of freedom in nodal x, y and z directions. It has plasticity, hyper elasticity, stress stiffening, creep, large deflection, and large strain capabilities (ANSYS 14, 2013). The only difference between SOLID185 and SOLID65 is that SOLID185 does not crack or crash. The geometry and node locations for this element type are shown in Figure (3.7).

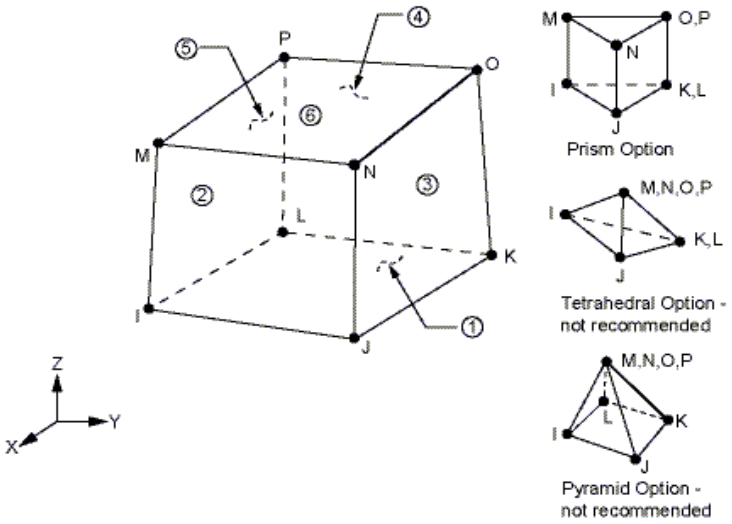

Figure (3.7): SOLID185 ELEMENT (ANSYS 14, 2013)

An elastic material property is considered for conventional steel. The thickness of the plate is taken as 20mm. The inputs required for a linear-elastic material are modulus of elasticity and Poisson's ratio which are specified as 200 GPa and 0.3, respectively.

3.3. Reinforcement-Concrete Interface

There are two approaches to simulate the bond behaviour between reinforcement and surrounding concrete. In the first approach, the node of concrete and the reinforcement share the same location with the same node numbering representing the perfect bond condition. This approach can be used if no slippage is expected between concrete and reinforcement. The second approach simulates the bond-slip between the reinforcement and the surrounding concrete. In analysis of prestressed concrete beam, slippage is likely to take place hence bond-slip relationship is taken into consideration. This can be achieved by introducing spring element between the concrete and the reinforcement nodes. Duplicate nodes are created along the length

of the reinforcement with a different node numbering at the same location as that of the concrete nodes. In other words, two nodes are created at the same location: one is for concrete and the other is for the reinforcement. These two nodes are connected by a spring element COMBIN14. The geometry and node locations for this spring element are shown in Figure (3.8).

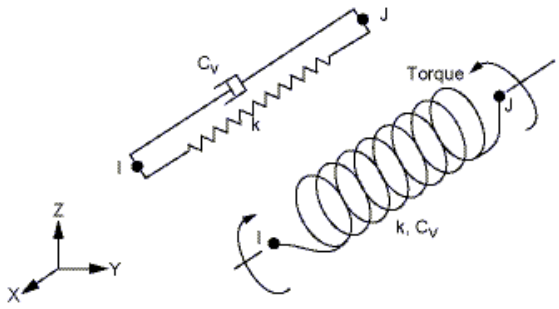

Figure (3.8): COMBIN14 ELEMENT (ANSYS 14, 2013)

This spring element has a longitudinal or a torsional capability in 1-D, 2-D, or 3-D applications. The longitudinal spring-damper option is a uniaxial tension-compression element with up to three translational degrees of freedom at each node (ANSYS 14, 2013). The only material property to be input to properly model this spring is the stiffness of the spring since damping is not present. To date, there has been no study on the bond-slip relationship of the CFCC tendon. The stiffness of the spring is considered to be 12000 N/mm based on the pull out tests conducted on CFPR bars by Cosenza et.al (1995) on the carbon fiber seven-wire strands.

3.4. Mesh Size selection

The selection of appropriate mesh size is very important in a FEA. Square or rectangular mesh is recommended to obtain the best result from SOLID65 element. The dimensions of the elements are chosen carefully so that the aspect ratio is within 2:1 ratio in three directions as suggested by ANSYS user's manual (2013) to avoid errors due to distortion effect. To obtain an optimum

mesh size, a number of trials are performed with different mesh sizes ranging from 75 mm to 15 mm and the beam with the span to depth ratio of 3.5 is selected for this purpose. The deflection at failure is plotted against the number of elements used in the analysis and is shown in Figure (3.9)

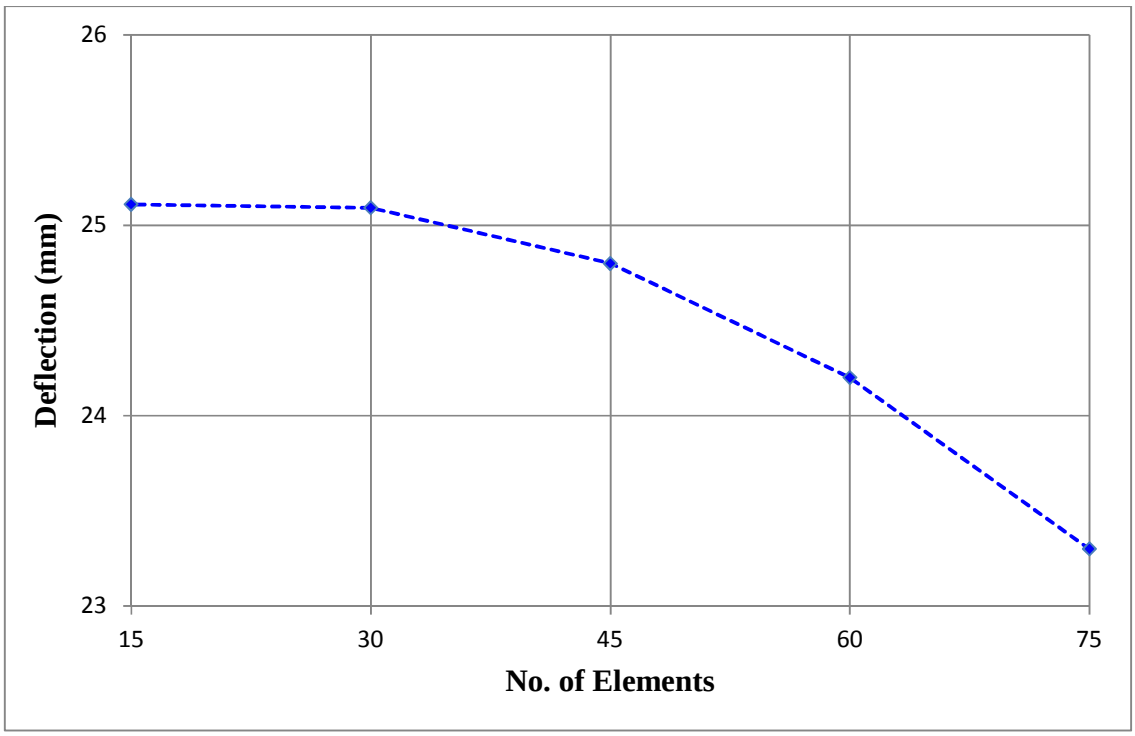

Figure (3.9): Convergence Test

The difference between the deflection values at failure of using 30 mm and 15 mm mesh size (50% decrease in size) is only 0.07%. Therefore, 30 mm is the most effective size. However, because of the restraints in the beam geometry such as the span and the loading location, it is not possible to use same mesh sizes for all the analyses .The actual mesh sizes considered in the analyses are shown in Table (3.3).

Table (3.3): Mesh Size

Beam Description	Mesh size (mm)
PR-3.5	30
PR-2.5	25
PR-1.5	28.3
PR-U	25

3.5. Geometry and Boundary Conditions

All of the beams considered in this study are simply supported over their span and of the same cross section and the same internal reinforcement. The cross section is symmetric in the geometry, the loading and the internal reinforcement about the vertical plane passing through the center of the beam. Therefore, only half of the beam is modeled. The beams are modeled such that the cross section is laid on global YZ plane in ANSYS which means global X-direction lies along the beam length and the global Y and Z directions orients along the depth and width of the beam, respectively (Figure 3.10). The cross section detail and other relevant information about the tested beams are presented in the next chapter. However, the cross-section of the beams is shown in Figure (3.10.) to better explain the boundary conditions. In order to simulate a simply supported boundary condition, a roller support is set at one end and a hinge support is assigned at the other end. This is achieved by restraining the vertical translation (Y) of all the nodes along the center line of the steel plate at the roller end and both the vertical (Y) and the horizontal (X) translations of all the nodes along the center line of the steel plate at the hinge end. Since half of the beam is modeled, all nodes located on the plane of symmetry are restrained against translation in transverse (Z) direction. The boundary conditions for the PR-3.5 beams are shown in Figure (3.10) and the same for the other beams can be found in the Appendix. In ANSYS, translation or displacement of nodes in a certain direction can be restrained by simply setting the displacement of those nodes to zero in that particular direction.

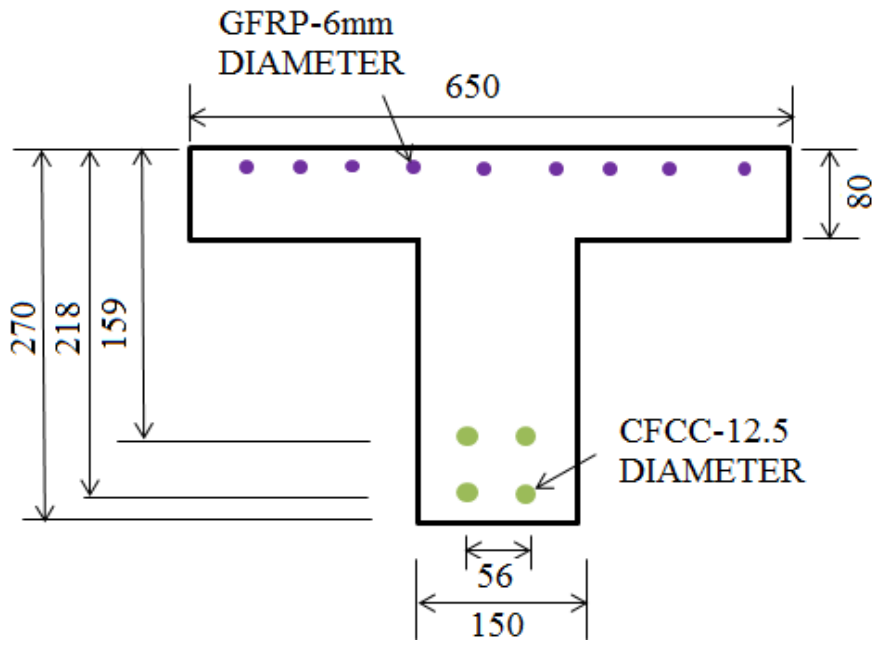
GFRP-6mm
DIAMETER
650
80
270
218
159
CFCC-12.5
DIAMETER
56
150

(a)

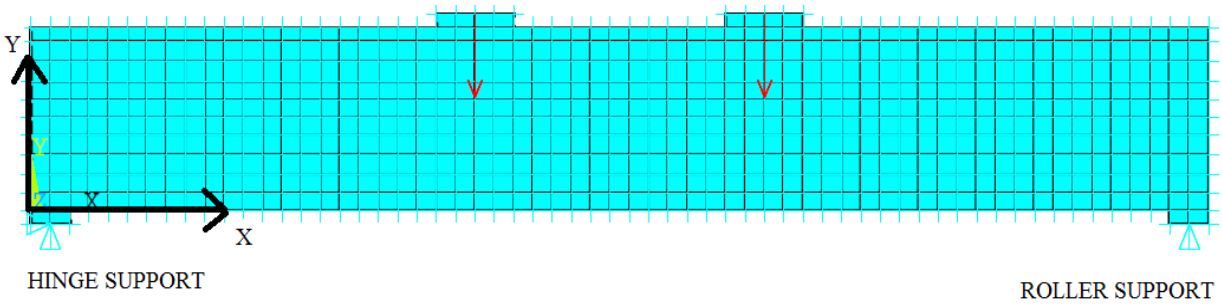
Y
X
HINGE SUPPORT
ROLLER SUPPORT

(b)

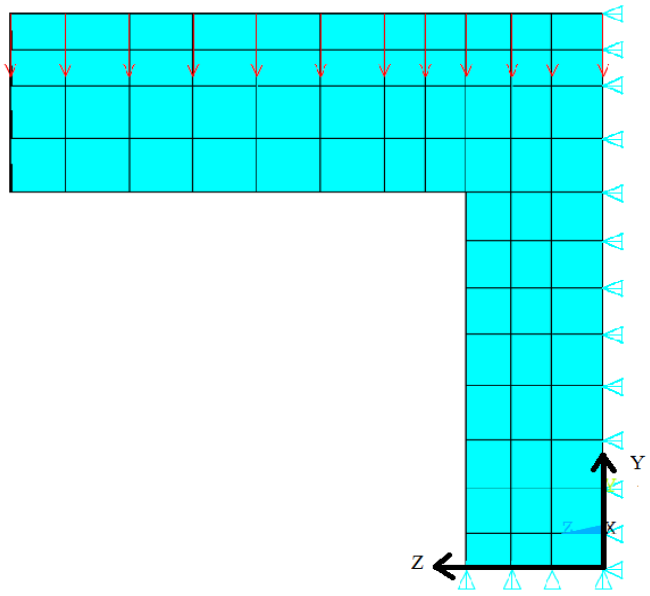

(c)

Figure (3.10): Boundary Conditions for the PR-3.5 beams a) Beam cross-section b) FEM model of beam elevation c) FEM model of beam cross-section

ANSYS has three phases to perform an analysis: preprocessing, solution and post processing phases. In the preprocessing stage, the model is created based on the given geometry and element types as discussed. In the solution phase, the loading and boundary condition are assigned to the problem and the model is analyzed. The last phase, the post-processing phase, is used to view the desired results of nodes and elements of interest.

3.6. Solution Control

There can be two types of non-linearity such as geometric non-linearity and material nonlinearity for a nonlinear problem. If a structure experiences large deformation, its changing geometric configuration can cause the structure to respond nonlinearly. Nonlinear stress-strain relationships are common cause of nonlinear structural behavior. The stress-strain response of concrete is nonlinear, whereas, the stress-strain curve for the FRP reinforcements is linear. In the current study, only material nonlinearity is encountered because of nonlinear stress-strain relationships of concrete. To model the concrete nonlinearity, ANSYS has built-in multi-linear isotropic material model. This model is used to input the concrete stress-strain curve as discussed in section 3.2.1.ANSYS employs the "Newton Raphson" approach to solve non-linear problems. In this approach, load is subdivided into a series of load increments. The load increments can be applied over several load steps. Before each solution, this method evaluates the out-of-balance load vector, which is the difference between the restoring forces (the loads, corresponding to the element stresses) and the applied loads. The program then performs a linear solution, using the out-of-balance loads, and checks for convergence. If convergence criteria are not satisfied, the out-of-balance load vector is re-evaluated, the stiffness matrix is updated, and a new solution is obtained. The iterative procedure continues until the problem converges based on specified convergence criteria. A number of convergence-enhancement and recovery features, such as line search, automatic load stepping, and bisection, can be activated to help the problem to converge. If convergence cannot be achieved, then the program attempts to solve with a smaller load increment. ANSYS has number of choices to define convergence criteria. It can be based on forces, moments, displacements, and rotations or combination of these items. Additionally, each

item can have different tolerance value. In summary, nonlinear analysis performed by ANSYS can be organized into the following three levels of operation (ANSYS 14, 2013).

- The first level consists of the load where the incremental applied loads are specified. Loads are assumed to vary linearly within load steps for static analysis.
- Each load step can be subdivided into number of substeps to apply the load gradually.
- At each substep, the program will perform a number of equilibrium iterations to obtain a converged solution.

The following section discusses the inputs provided to the FE models to perform the nonlinear analysis.

An incremental load of 30 kN in each load step (LS) is applied to the beam to failure. This load is divided equally and applied to all the nodes at the centre line of the steel plate. The load steps are subdivided into a number of substeps. The maximum and minimum substeps are specified as 200 and 100, respectively. The automatic time stepping is set on for faster convergence. At the end of each load step, the stiffness matrix of the model is adjusted to encompass the non-linear changes in the structural stiffness before moving on to the next load step. Newton-Raphson technique is selected in the iteration to update the model stiffness

In this study, the convergence criterion is based on displacements and the tolerance value is set as 5%. The first loading step is used to transfer the prestressing force from the strands to the surrounding concrete. The incremental loading is applied from the second load step to the beam failure.

Chapter 4

ANALYSIS OF PRESTRESSED CONCRETE BEAM

4.1. General

In this chapter, the geometry and the material properties of the tested beams are presented and numerical analysis of the beams is reported. The FE models of the beams are constructed in ANSYS 14 in line with the previous chapter. The results of the models are compared with the experimental data for validation. Finally, parametric studies are conducted to investigate the influences of prestressing forces and the a/d ratios on the shear capacity of the beams. The shear capacities obtained from the FEA for different a/d ratio are also compared with the North American codes.

4.2. Experimental Data

The experimental results used for the FEA validation in this study are taken from the tests conducted by Nabipaylashgari (2012) at University of Manitoba. In the experiment, the beams were divided into four groups. Two specimens were tested in each group. The first three groups had different a/d ratio and all the beams in these groups were subjected to four points bending. The beams in the last group were subjected to uniformly distributed load. The beams considered in this study had no shear reinforcement. The cross section and internal flexural reinforcement of all the beams were the same and is shown in Figure (4.1).

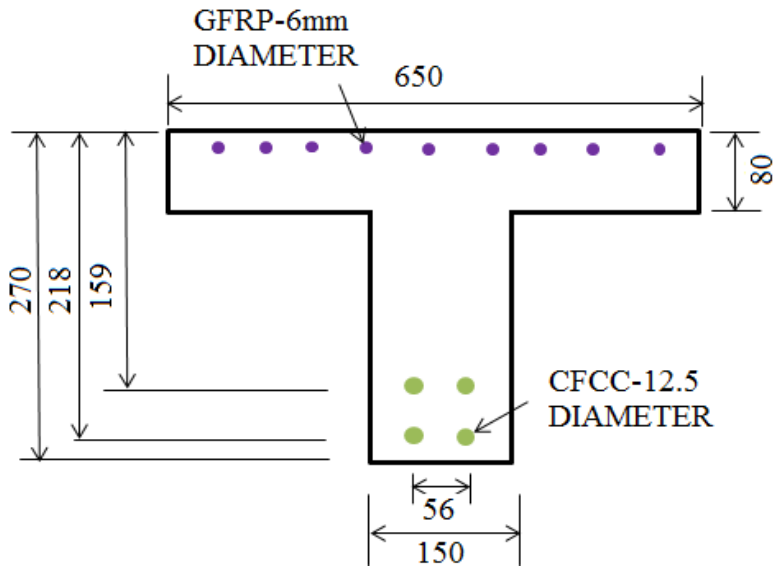

Figure (4.1): Cross-section details of the Experimental Beams

Four 12.5 mm CFCC prestressing strands were used as the flexural reinforcement and they were designed such that the beams will fail in shear rather than in flexure. The flange reinforcement consisted of nine 6 mm GFRP bars.

The elevations of each group are presented in Figure (4.2) where "a" refers to the shear span and "L" refers to the span of the beam. The beams were simply supported over the span and loaded to failure.

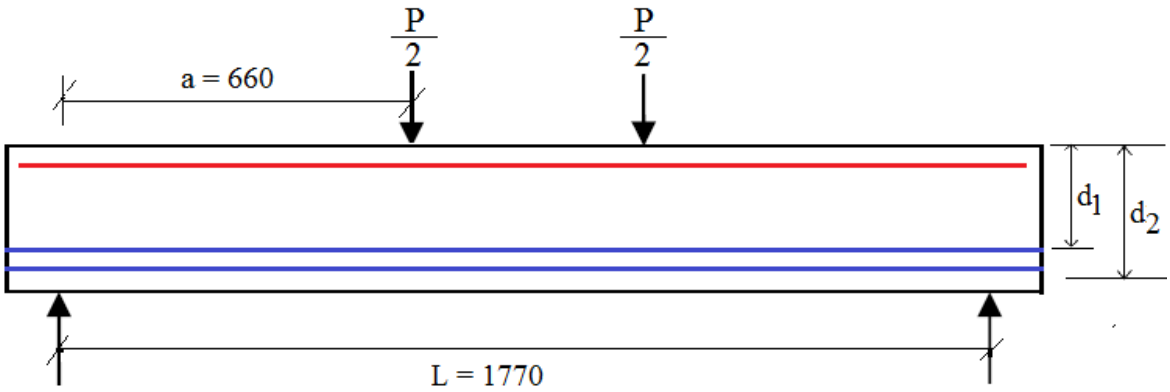

(a)

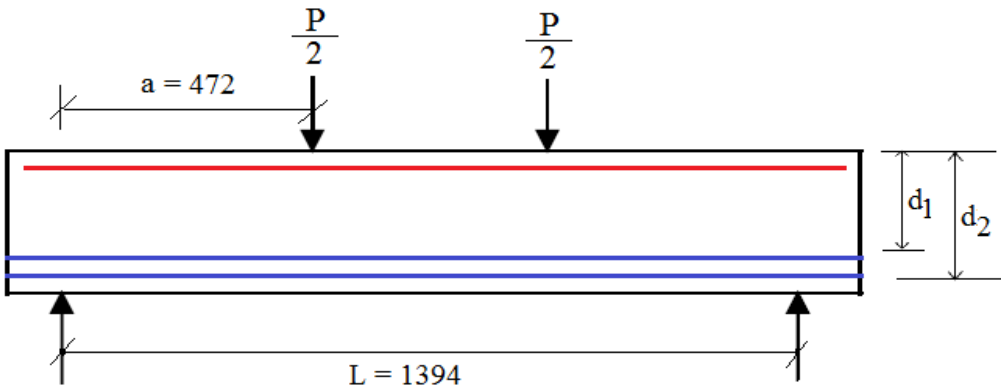

(b)

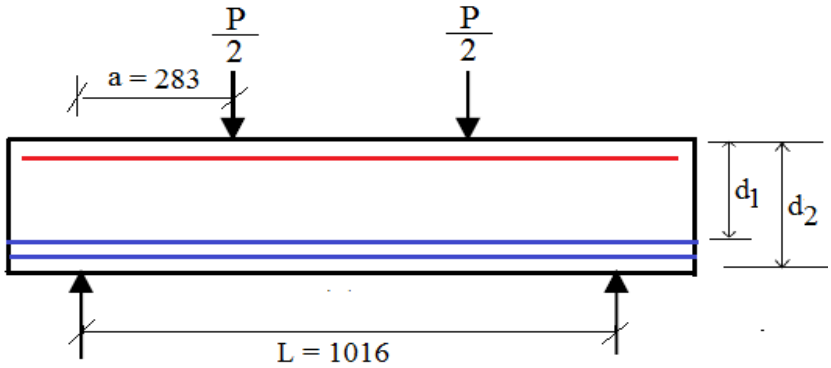

(c)

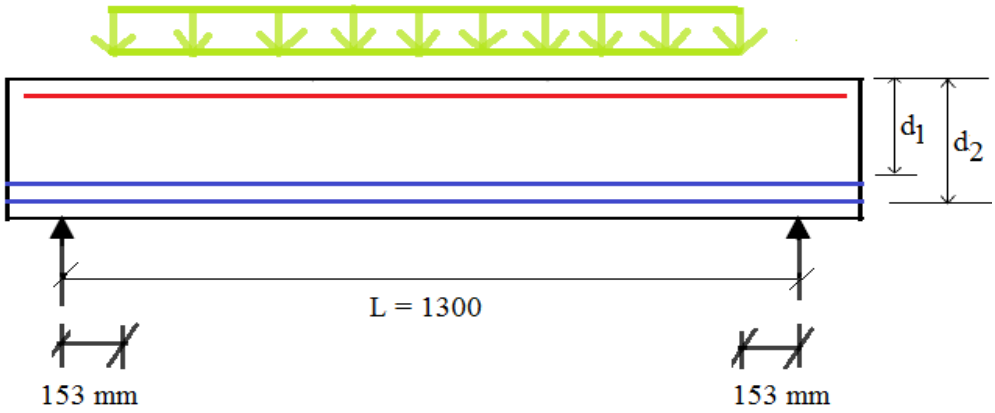

(d)

Figure (4.2): Elevation of the Experimental Beams a) PR-3.5 b) PR-2.5 c) PR-1.5 d) PR-U

The dimensions of "a" and "L" are also given in Table (4.1).

Table (4.1): Geometry of the Tested Beams

Beam ID	a (mm)	d_1 (mm)	d_2 (mm)	L (mm)	a/d ratio	Type of Loading
PR-3.5	660	159	218	1770	3.5	Two Point Loads
PR-2.5	472	159	218	1394	2.5	Two Point Loads
PR-1.5	283	159	218	1016	1.5	Two Point Loads
PR-U	-	159	218	1300	-	Uniform Load

The material properties of concrete and of the reinforcement are presented in Table (4.2) and Table (4.3), respectively.

Table (4.2): Concrete Properties of the Tested Beams

Beam ID	f'_c (MPa)	f_{cr} (MPa)	E_{cexp} (MPa)
PR-3.5	48	3.2	28888
PR-2.5	47	3.6	24704
PR-1.5	47	3.34	30227
PR-U	49	3.14	24827

Table (4.3): Reinforcement Properties of the Tested Beams

Description	Material	Diameter(mm)	Cross-section (mm^2)	f_{pu} (MPa)	E (GPa)
Prestressing Strand	CFCC	12.5	76	2047	136
Flange Reinforcement	GFRP	6	31.67	827	40.8

The CFCC were initially prestressed to 51% of the ultimate stress which produced camber along the length of the beams. The final prestressing forces were recorded after all the losses between the day when the jacking stress was released and the day when the experiment was conducted for

all the specimens. The strain corresponding to the final prestressing force is shown in Table (4.4). All the beams failed in shear and the failure loads are listed in Table (4.5).

Table (4.4): Prestressing Forces of the Tested Beams

Beam ID	Prestressing Force F_{pe}(kN)	Initial Strain
PR-3.5	267	0.0064600
PR-2.5	245	0.0059259
PR-1.5	255	0.0061678
PR-U	255	0.0061678

Table (4.5): Failure load of the Tested Beams

Beam ID	Level	Description	Load at Failure P_{exp}(kN)	Mode of Failure
PR-3.5	PR1-3.5	Specimen 1	298	Shear
	PR2-3.5	Specimen 2	293	Shear
PR-2.5	PR1-2.5	Specimen 1	372	Shear
	PR2-2.5	Specimen 2	364	Shear
PR-1.5	PR1-1.5	Specimen 1	655	Shear
	PR2-1.5	Specimen 2	666	Shear
PR-U	PR1-U	Specimen 1	598	Shear
	PR2-U	Specimen 2	601	Shear

4.3. Model Verification

In this section, the analysis results of the four groups of beams considered are presented and compared with the test results. The isometric view and the deflected shape at failure are only shown for the PR-3.5 beams. The isometric view and the deflected shape for the other beam groups are included in the Appendix. For any concrete beam analysis, load-deflection behavior is considered as the key response. In order to verify the FE models, the load-deflection response is primarily taken into consideration. In the tests, the strain gauge was mounted on the top flange of

the beams at mid span location to record the maximum compressive strain. A comparison of the concrete strain predicted by the FE models and the test results is also presented. Deflections are also calculated from section analysis based on the curvature obtained from the strain profile at mid-span. The same is also presented in the load-deflection plots of the respective beams. The following subsection discusses the validation of the FE models.

4.3.1. PR-3.5 Beams

The isometric view of the PR-3.5 beam modeled in ANSYS is presented in Figure (4.3).

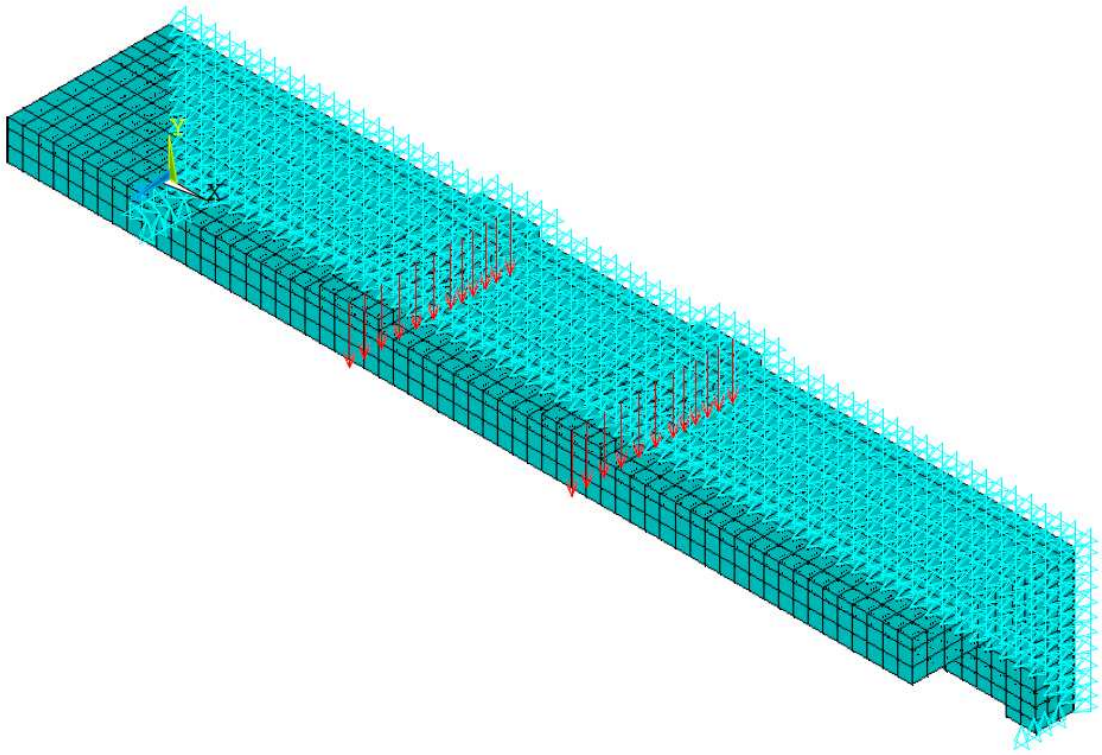

Figure (4.3): Isometric View of the PR-3.5 beam modeled in ANSYS

The analysis result shows that the beam fails in shear compression. The load at failure is 313 kN and the corresponding deflection is 28 mm. The deflected shape at failure for the beam is shown in Figure (4.4).

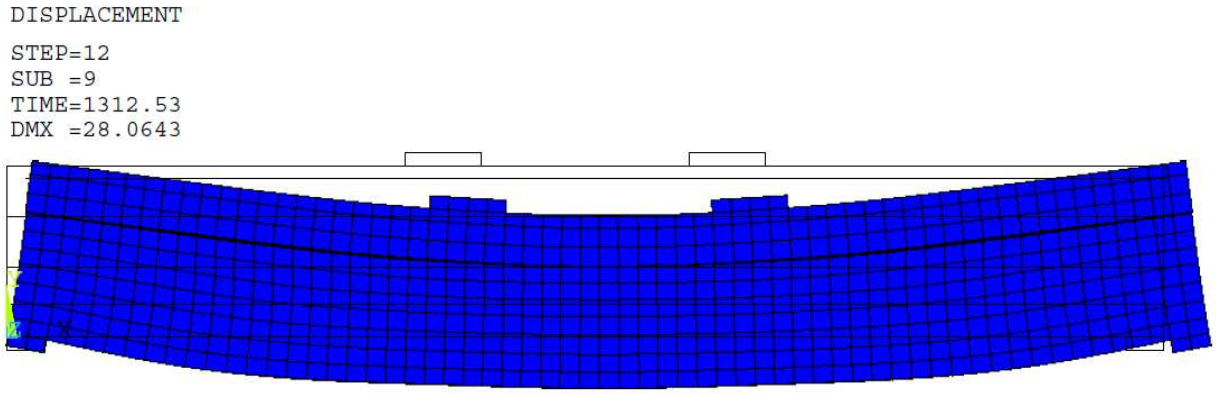

Figure (4.4): Deflected Shape of the PR-3.5 beam at failure

A comparison of the load-deflection response between the FEA and the test results for the PR-3.5 beam is shown in Figure (4.5). The failure load predicted by ANSYS is 5.9% more than the failure load obtained from the test results. It can be seen from the figure that the post cracking behavior is captured accurately.

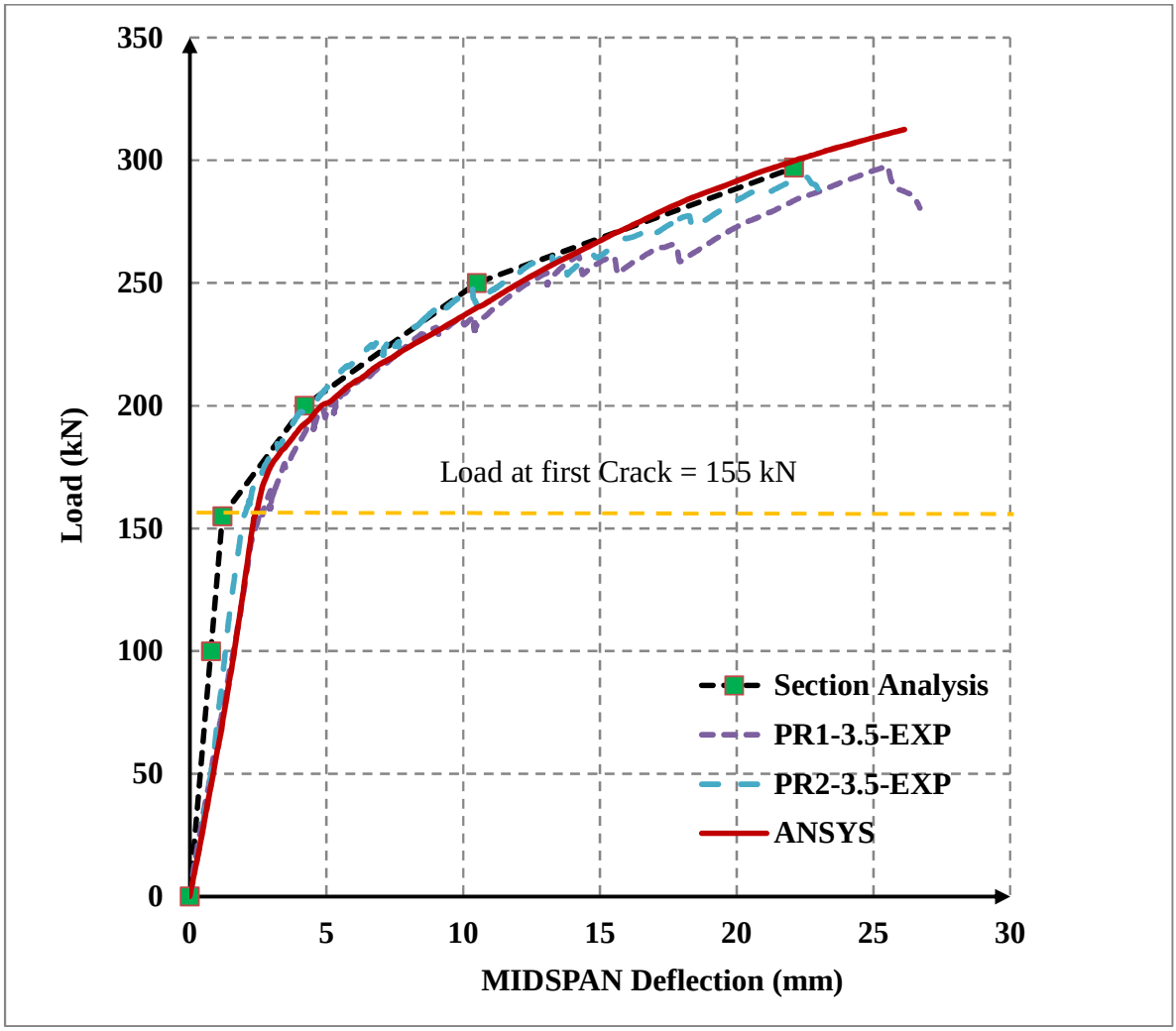

Figure (4.5): Load Deflection Response of the PR-3.5 Beams

Figure (4.6) presents a comparison of the concrete strain predicted by the FE models and the measured values. It can be seen that the model is able to predict the similar response as that of the experimental result. The difference in the two results is found to be less than 15%.

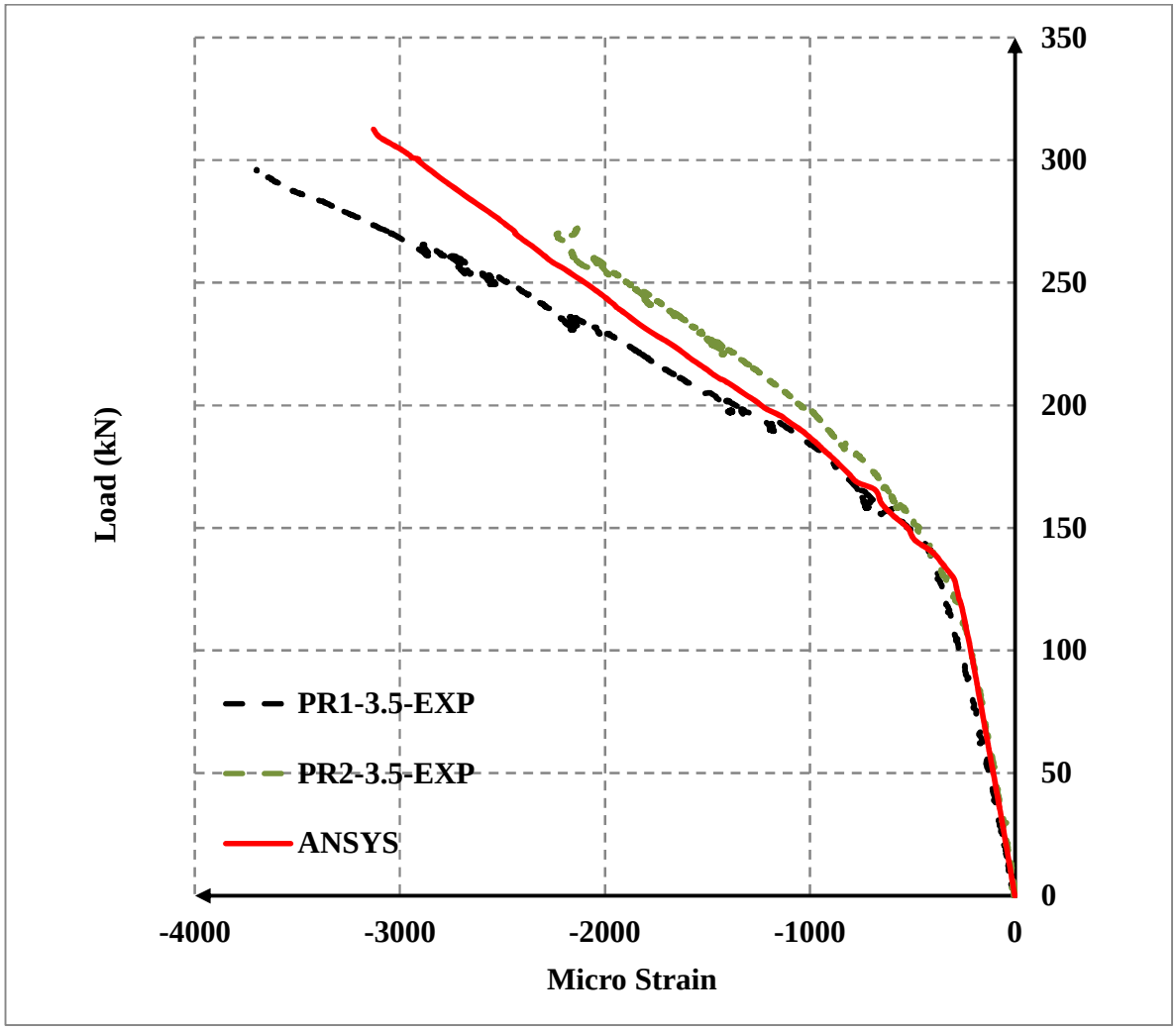

Figure (4.6): Concrete Compressive Strain Plot for the PR-3.5 Beams

4.3.2. PR-2.5 Beams

A comparison of the load-deflection response between the FE model and the experimental results for the PR-2.5 beam is shown in Figure (4.7). The mode of failure of this beam is shear compression failure. The failure load predicted by the FE model is 379 kN which is 3 % higher than the failure load as recorded during the test. This indicates that the FE model is able to simulate the test results with acceptable degree of accuracy.

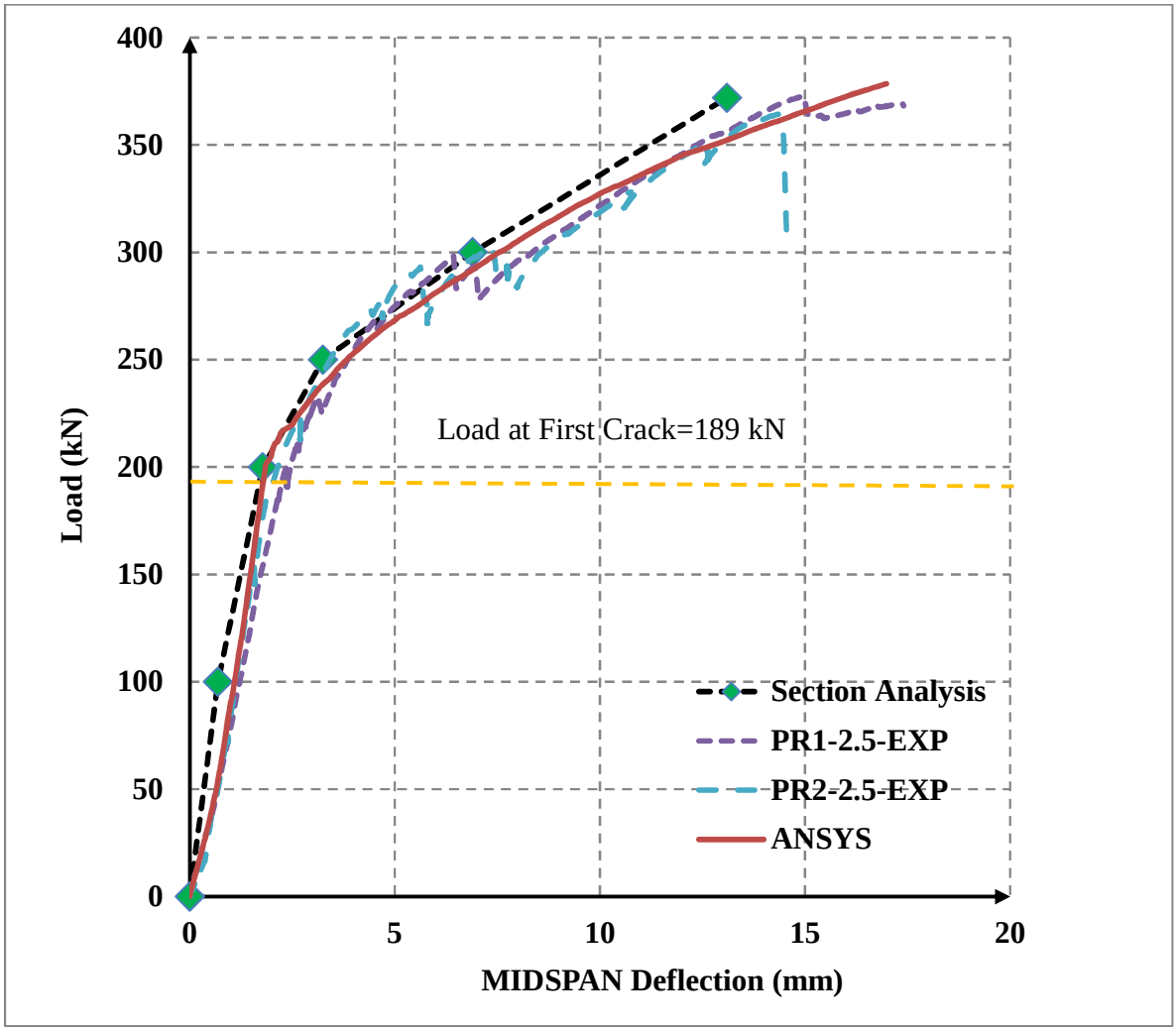

Figure (4.7): Load Deflection Response of the PR-2.5 Beams

Load versus concrete strain at the mid span is compared in Figure (4.8). The figure shows a similar trend between the numerical and test results. The ultimate strain at failure predicted by ANSYS is 14.7% lower than results measured in the tests.

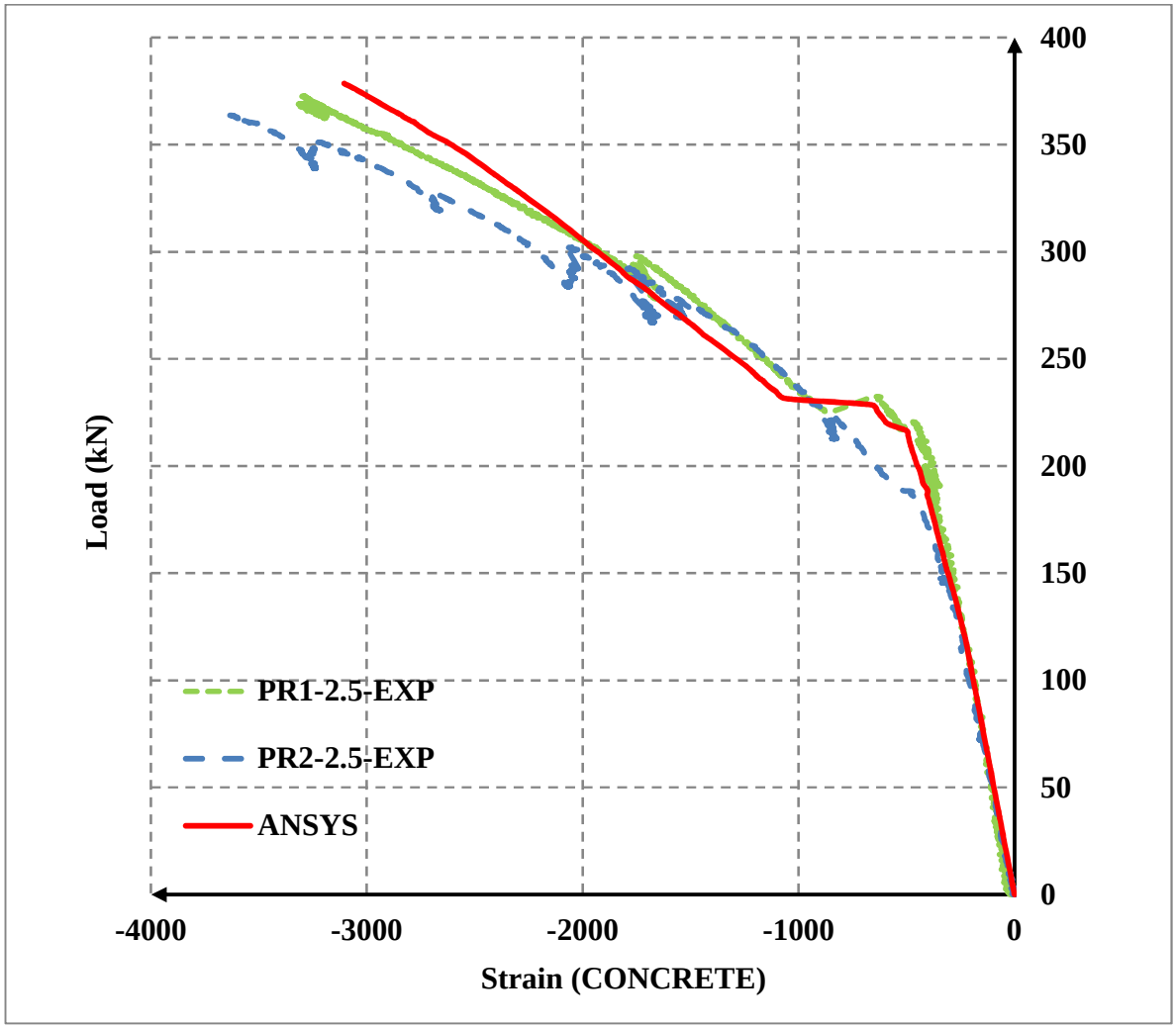

Figure (4.8): Concrete Compressive Strain Plot for the PR-2.5 Beams

4.3.3. PR-1.5 Beams

Figure (4.9) shows a comparison of the load-deflection response between the numerical model and the experimental results for the PR-1.5 beams. The shear failure load predicted by ANSYS is 689 kN which is 3.4% more than the failure load from the test results. However, the FE model predicts a stiffer response in the elastic range (the loads ranging between 35 kN and 300 kN) and a less stiff response in the inelastic range. The PR-1.5 beams are considered as deep beams because the a/d ratio is less than 2.5 and the span of the beam is only 1016 mm. The load is

transferred from the loading point to the support by a compression strut and this phenomenon is known as arch action. The difference between the deflection estimated by FEA and the test result at 300 kN applied load is 1.6 mm. A significant amount shear deformation took place due to the load transfer by arch action. The FE model could not simulate the shear deformation which is the reason of stiffer load-deflection response in the elastic region. However, the ultimate load and deflection are well estimated by the FE model.

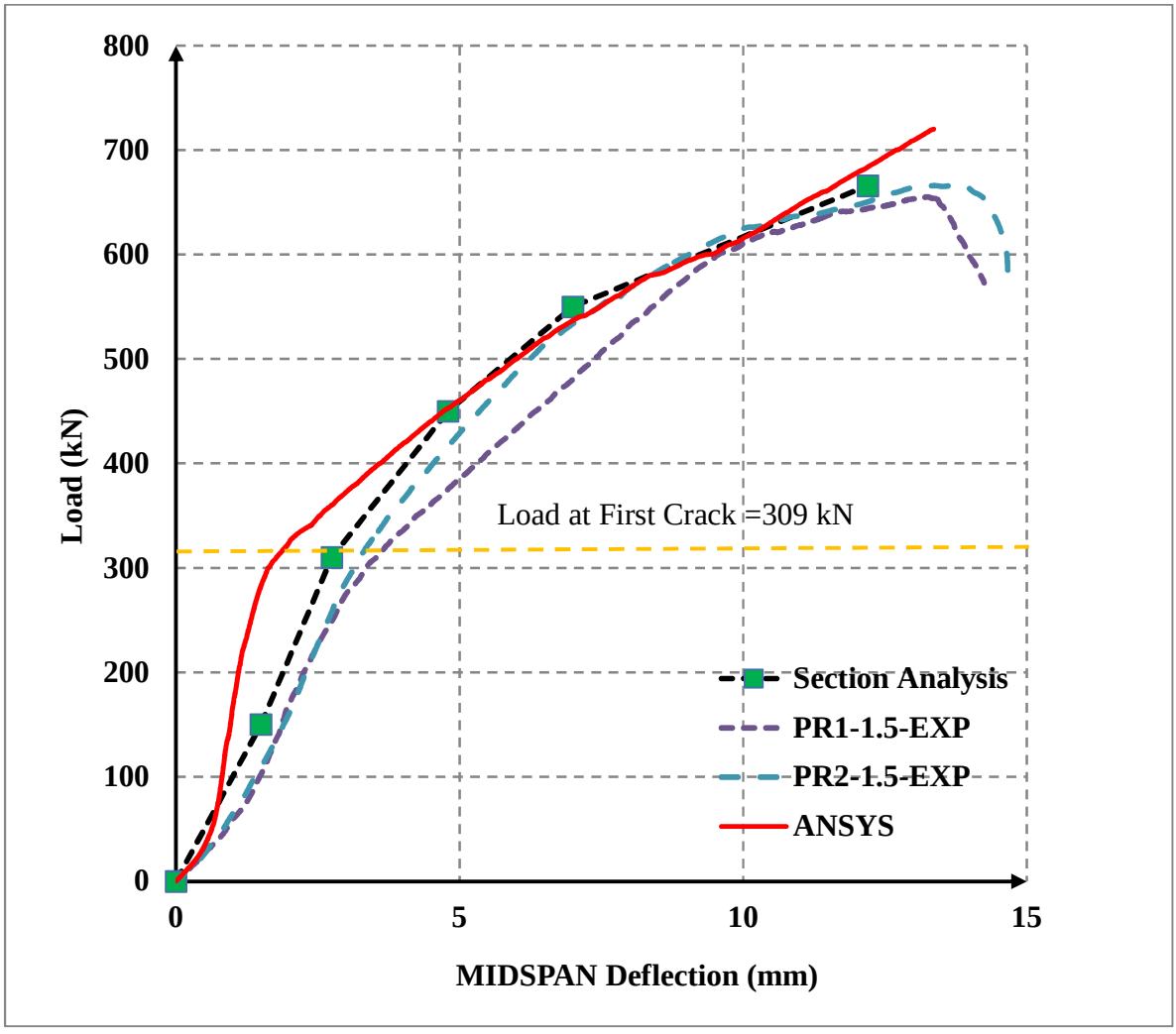

Figure (4.9): Load Deflection Response of the PR-1.5 Beams

The concrete strains at the mid-span location of the PR-1.5 beams are plotted in Figure (4.10). It can be seen that the FE model predicts similar trend of the concrete strain response as that of the tested results. However, the maximum strain obtained from the experiments was 17% higher than that from the FEA.

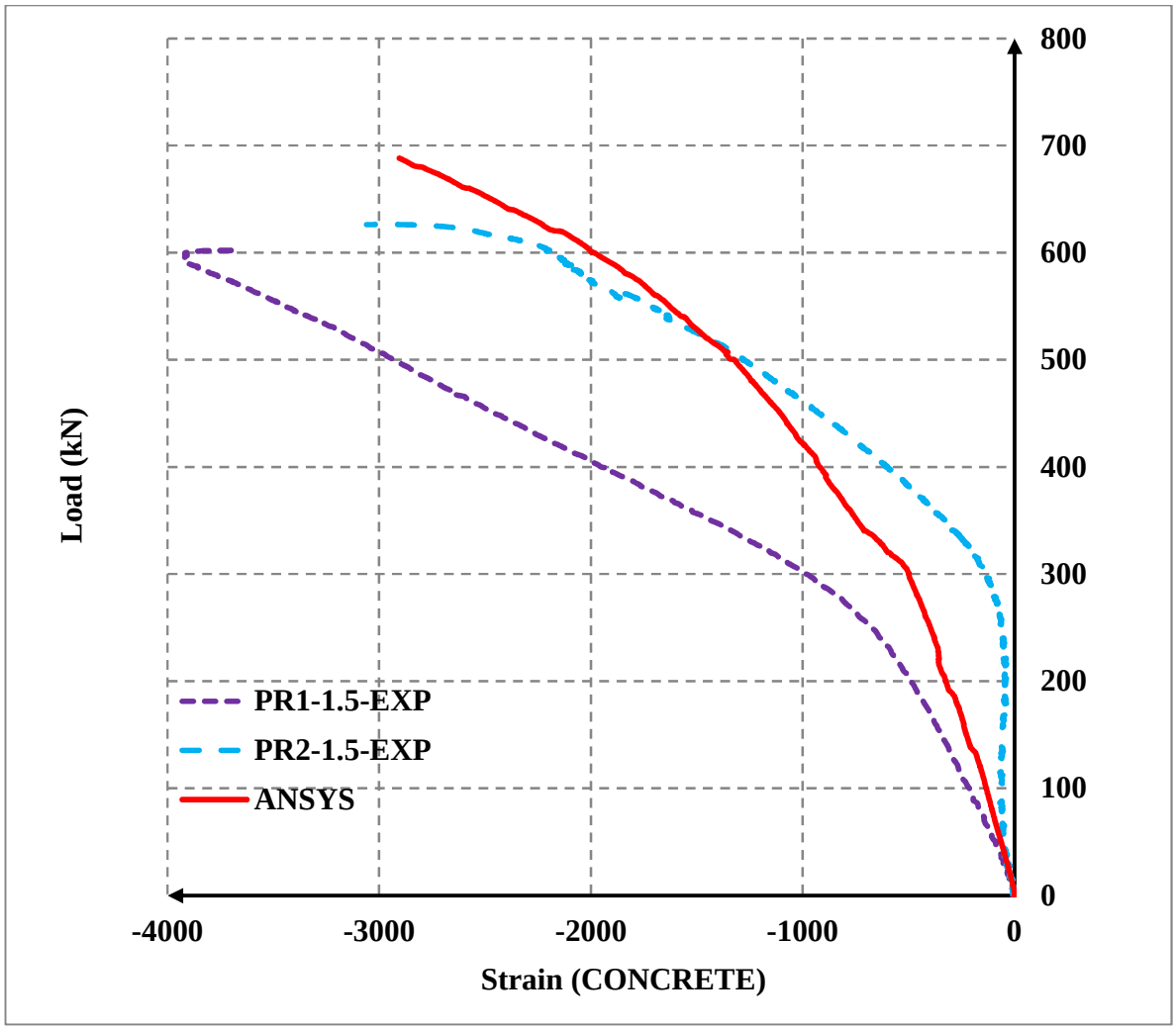

Figure (4.10): Concrete Compressive Strain Plot for the PR-1.5 Beams

4.3.4. PR-U-Beams

A comparison of the load-deflection response between the ANSYS results and the test results for the PR-U beam is shown in Figure (4.11).The mode of failure for this beam is shear compression

failure as well. The failure load predicted by ANSYS is 613.3 kN which is 2% more than the measured failure loads. From the figure, it can be seen that the experimental response of the specimen 1 is better predicted by the FE model than the specimen 2. However, the analytical result is in the acceptable range for both the specimens.

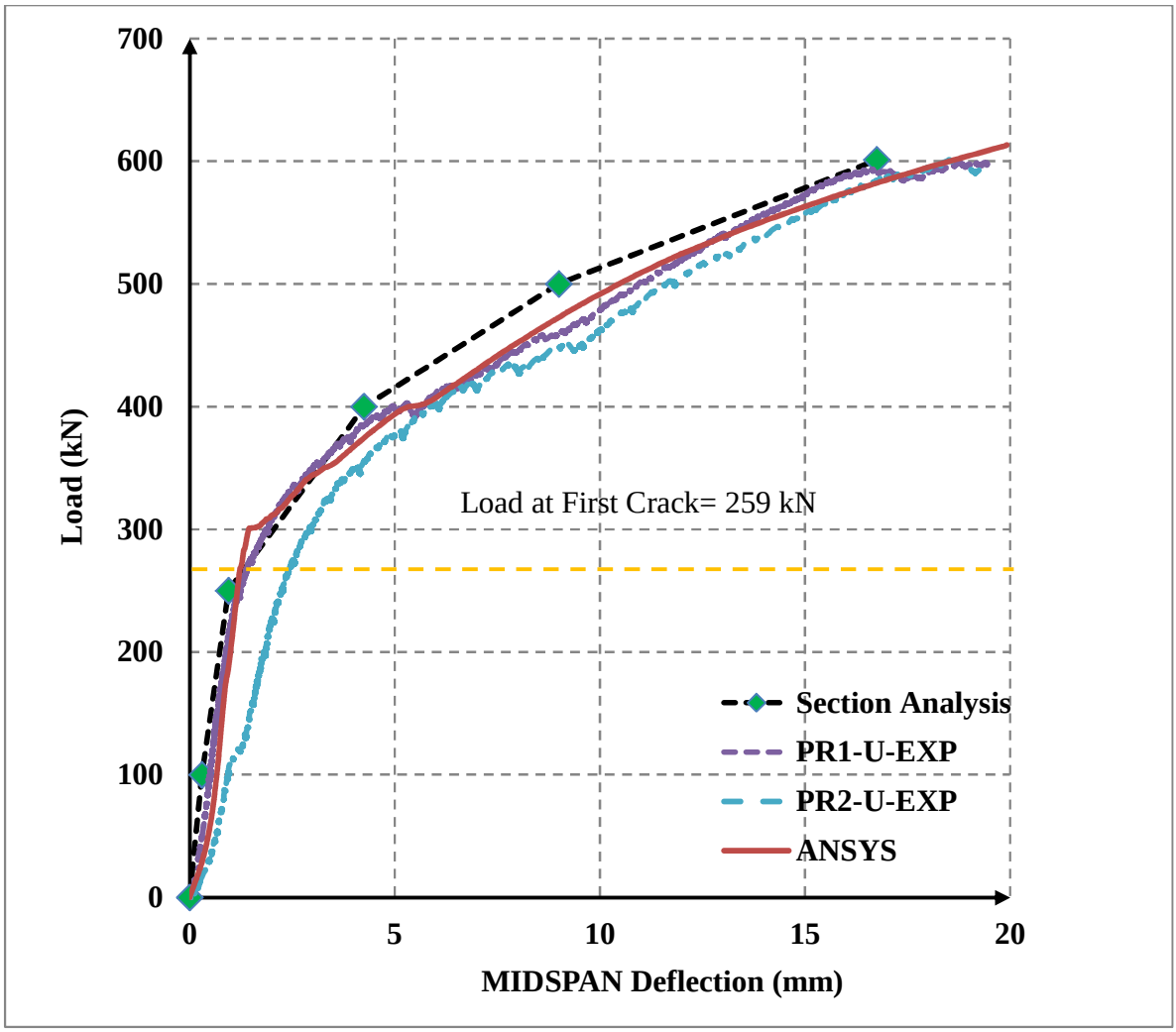

Figure (4.11): Load Deflection Response of the PR-U Beams

Load versus concrete strain at the mid span is shown in Figure (4.12). The figure shows a similar trend between the numerical and test results. The ultimate strain at failure predicted by ANSYS is 21% lower than results recorded in the tests.

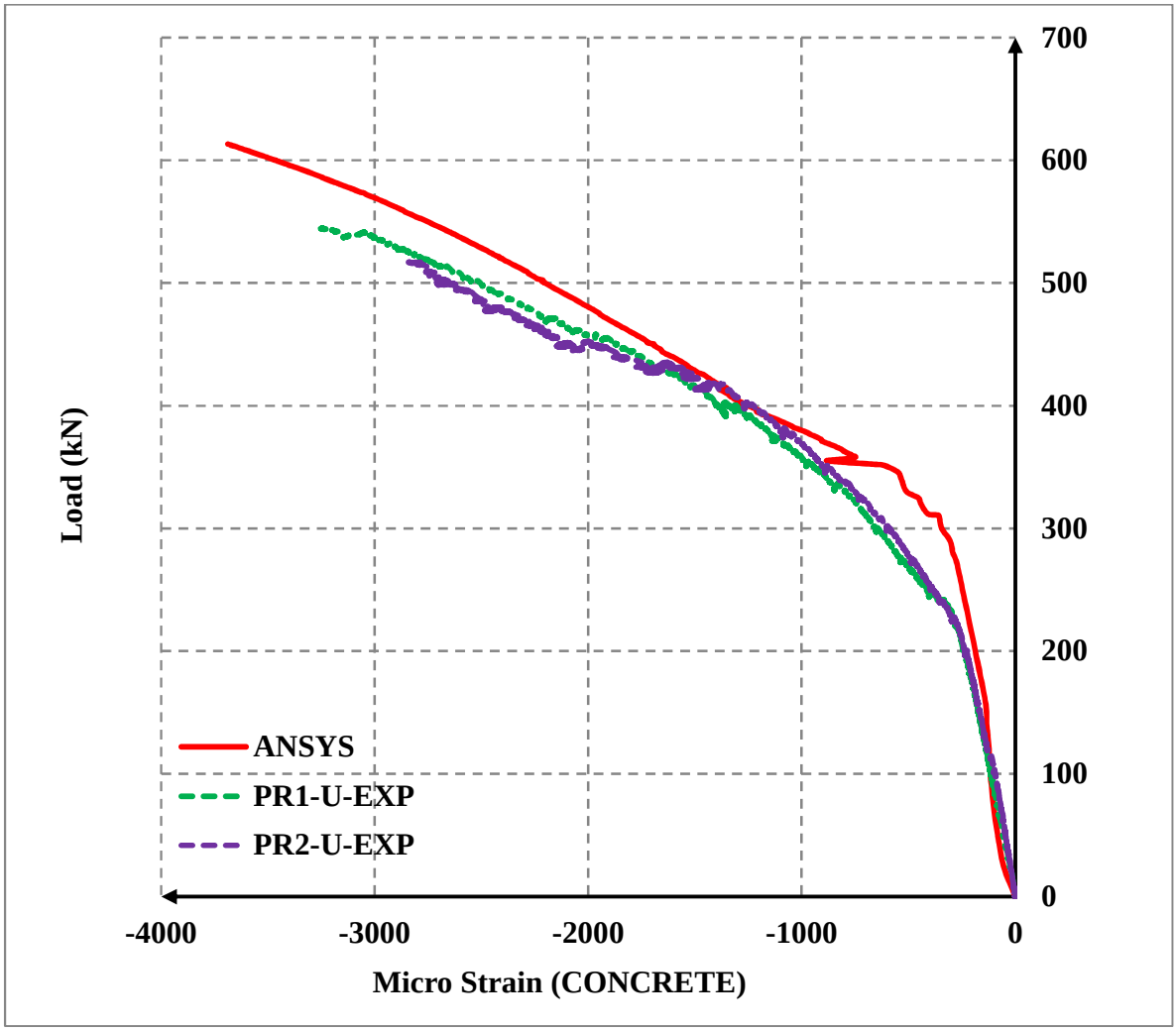

Figure (4.12): Concrete Compressive Strain Plot for the PR-U Beams

4.4. Parametric Study

As seen in the previous section, the constructed FE models for the PR-3.5, PR-2.5, PR-1.5 and PR-U beams are able to predict the failure loads and the failure modes very closely to what were observed in the experiments. A total of three additional a/d ratios will be generated: 2.0, 3.0, and 4.0. The validated FE models will be used to investigate the influence of the a/d ratios on the failure loads. The FE model for the PR-3.5 beams will be used to construct the numerical models for the a/d ratios of 4.0 and 3.0, and these beams are designated as the PR-4.0 and the PR-3.0

beams, respectively. The only modification made in the model is to move the position of the applied loads to result in the desired a/d ratios. Similarly, the FE model for the PR-2.5 beam will be used to construct the analytical model for the PR-2.0 beam which has the a/d ratio of 2.0.

4.4.1. Influence of Shear Span-To-Depth Ratios on the Shear Capacity

Figure (4.12) shows a variation of the shear capacities with different a/d ratios predicted by the FE models and the test results. It is observed from the plot that the shear capacity decreases with the increase in the a/d ratios. The increase in shear capacities is much perceptible for lower a/d ratios. The increase in the shear capacity is 87% when the a/d ratios decreased from 2.5 to 1.5. However, there is only 32% higher capacity observed when the a/d ratios varied from 4.0 to 2.5. This is because a significant portion of the applied load is transmitted directly to the support by an inclined compression strut when a/d ratio is less than 2.5. This mechanism is frequently referred to as arch action (MacGregor et al. 2000).

The shear capacities from the latest shear design formulas from the North American codes are also included in the Figure (4.12). The three North American design codes considered in this study are the Prestressing Concrete Structures with FRP Tendons (ACI 440.4R-04), the Canadian Highway Bridge Design Code (CSA-S6-10) and the Design and Construction of Building Structures with Fiber-Reinforced Polymers (CSA-S806-12). The shear design formulas from the above design codes are presented in the Appendix-E. The CSA-S806 predicts the ultimate capacity for a/d= 2.5 better than other design codes. For beams with a/d ratios greater than 2.5, the bridge code CSA-S6-10 gives better results. ACI 440.4R-04 yields the most conservative shear capacities compared to other design codes. A summary of the shear capacities obtained from the FEA and from the North American codes and the ratio of FEA prediction to the calculated design capacities are presented in Table (4.6).

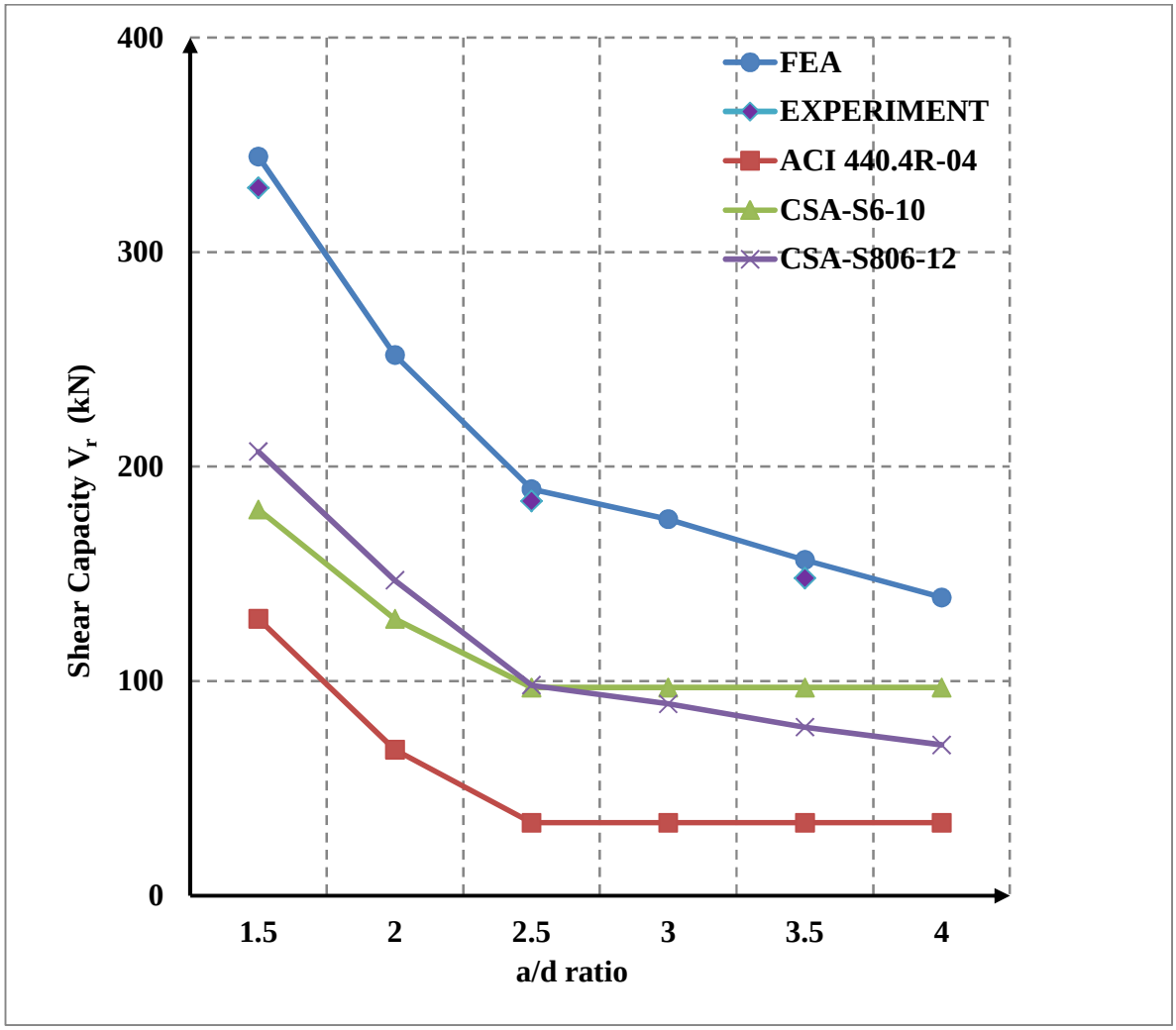

Figure (4.13): Shear Capacity Prediction for Different a/d Ratios and Comparison with the North American Codes

It is worth to note that the trend of the plots for shear capacities predicted by FEA and CSA-S806-12 for different a/d ratios is very similar. An average safety margin of 1.8 is found between the shear capacities for a/d ratios 1.5 to 4.0.

Table (4.6): Comparison of Shear Capacities from the FEA and North American Codes

Beam ID	Shear Capacity (kN)				Ratio of FEA to Theoretical Shear Capacity		
	FEA	ACI-440.4R-04	CSA-S6-10	CSA-S806-12	ACI-440.4R-04	CSA-S6-10	CSA-S806-12
PR-1.5	345	129	180	207	2.7	1.9	1.7
PR-2.0	252	68	129	147	3.7	2.0	1.7
PR-2.5	190	34	97	98	5.6	2.0	1.9
PR-3.0	176	34	97	89	5.2	1.8	2.0
PR-3.5	157	34	97	79	4.6	1.6	2.0
PR-4.0	139	34	97	70	4.1	1.4	2.0

4.4.2. Influence of Shear Span-To-Depth Ratios on Moment Capacity

The variation of shear failure moment capacities as obtained from the FEA and the experiment results are plotted against a/d ratios in Figure (4.14). The shear failure moment is calculated from the shear failure load multiplied by the respective shear span. The horizontal line shows the theoretical moment capacity as obtained from the section analysis. It can be seen from the graph, the shear moment capacity reduces from a/d ratio 1.5 to 2.5 and it again increases from a/d 2.5 onwards. The minimum shear failure moment is noticed at a/d ratio equal to 2.5. Similar curve was obtained from the experiments on reinforced concrete beams by the past researchers (Leonhardt et al. 1976, Joint Report by ASCE-ACI Task Committee 426, 1973). For very short beams, with a/d ratio 0 to 1, inclined crack is developed along the line joining the load and support point. These cracks eliminate the horizontal shear flow from the longitudinal reinforcement to the compression zone of the beam. Load is transferred by arch action from loading point to the support by compression strut and the reinforcement acts as tension tie from support to support. Short beams with a/d ratio between 1.0 and 2.5, carry load partly by beam action and partly by arch action after redistribution of the internal forces. In other words, it is the

transition stage between the beam action and arch action mechanism which reduced the shear moment capacity. The behavior of slender beams with a/d ratio greater than 2.5 is different and load is entirely carried by beam action. However, the developed inclined cracks propagate through the beam and with further increase in load at some stage it becomes unstable the beam fails at inclined crack before reaching its full flexural capacity (MacGregor et al. 2000, Joint Report by ASCE-ACI Task Committee 426, 1973). In Figure (4.14), the shear failure moment capacity is reduced from 1.5 to 2.5 because of transition state from arch action to beam action. As the slenderness of the beams increases from a/d= 2.5 onwards, the shear moment capacity is increasing toward the flexural moment capacity as reflected in Figure (4.14). Beam having a/d ratio greater than 6 generally fails in flexure before formation of the inclined cracks and it was confirmed by past researchers (Leonhardt et al. 1976, Joint Report by ASCE-ACI Task Committee 426, 1973). The difference between the flexural moment capacity and shear failure moment capacity is the reduction in strength due to shear.

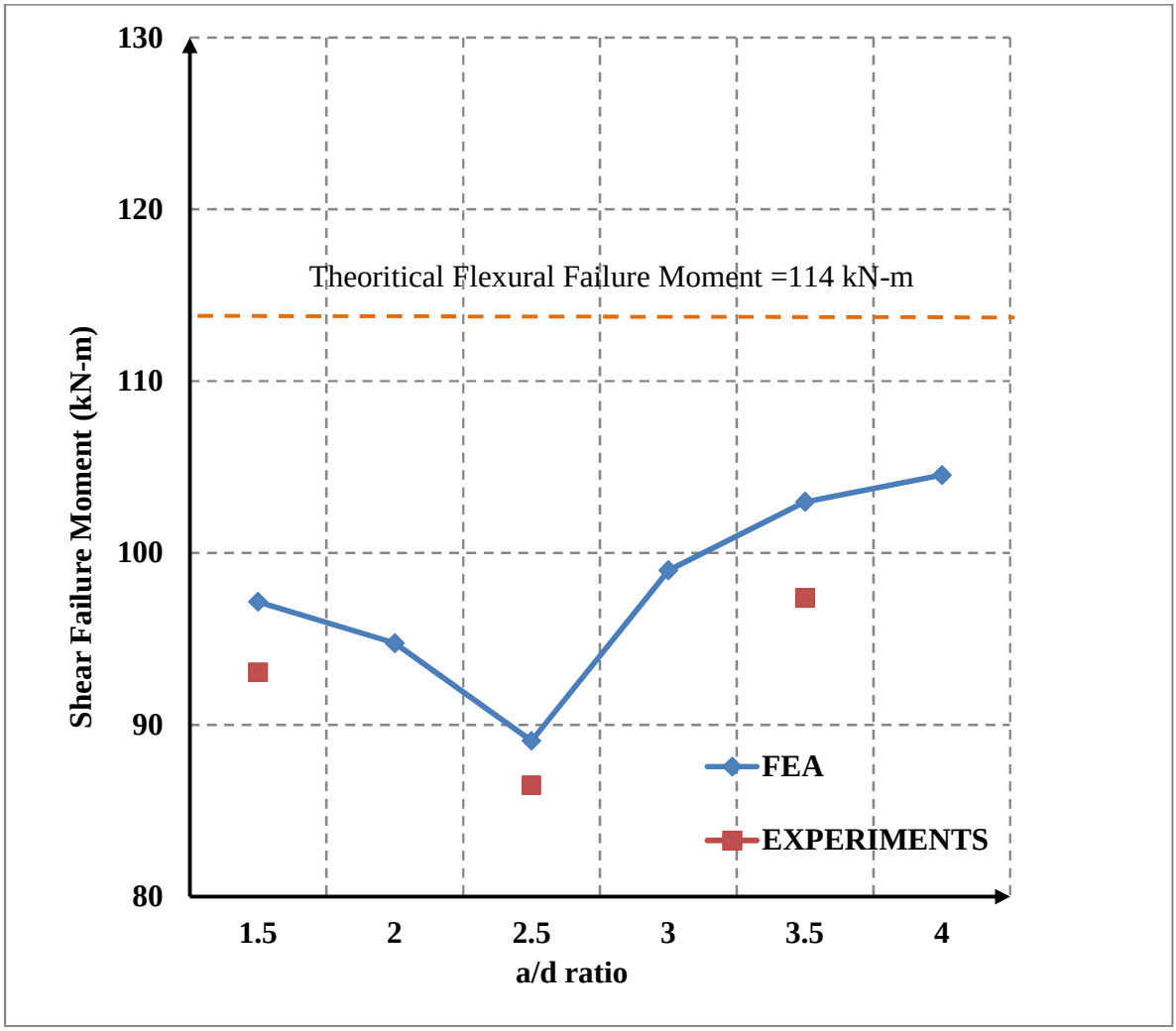

Figure (4.14): Variation of Shear Failure Moment Capacities with a/d Ratios

4.4.3. Influence of the Levels of Prestressing on the Shear Capacities

To investigate the influence of the prestressing forces on the shear capacity of the beam, the prestressing forces are varied for a fixed a/d ratio. The maximum limit of the prestressing stress at transfer condition is 65% of the rapture stress of the tendons (CSA-S806-12). Therefore, the maximum effective prestressing force that can be applied to CFCC is 51% of the ultimate capacity of the tendon considering average loss of 22% which was observed in the experiments. The average final prestressing force for the beams was reported at 41%. Therefore, the variations

of prestressing force of 51% and 30% of the ultimate capacity of the CFCC are considered in the FEA as an upper limit and a lower limit, respectively.

The shear capacities of seven beams: PR-1.5, PR-2.0, PR-2.5, PR-3.0, PR-3.5, PR-4.0 and PR-U, are obtained from the FEA for the different levels of prestressing force and are summarized in Table (4.7). It can be seen that the shear capacity increases with an increase in the prestressing forces. The average increase in the shear capacity when the level of prestressing forces varied from 30% to 41% (37% increased in the prestressing force) is found to be 5.1%. Similarly, the average increase in shear capacity is noticed as 11.3% when the prestressing level changed from 30% to 51% (70% increased in the prestressing force). It can be concluded that the increase in the shear capacity is almost linear when the prestressing level is varied.

Table (4.7): Comparison of Shear Capacities for different levels of Prestressing Force

Beam ID	Change In Prestressed level 37(%)		Change In Prestressed level 67(%)	
	Shear Capacity (kN)	Percentage Increased (%)	Shear Capacity (kN)	Percentage Increased (%)
PR-1.5	344.5	4.6	362	9.9
PR-2.0	252	4.8	269	11.9
PR-2.5	189.5	5.9	205.5	14.8
PR-3.0	175.5	5.1	188	12.6
PR-3.5	156.5	5.0	164.5	10.4
PR-4.0	139	4.9	144.5	9.1
PR-U	306.6	5.7	321	10.7

A comparison of shear capacity with the increase in the a/d ratio for different level of prestressing force is also presented graphically in Figure (4.15). As seen from the plots, the variation of the shear capacities for different degree of prestressing level varies in similar manner and the difference observed in the capacities is due to the variation of the prestressing force. It is noted that the effect of prestressing force is minimal for different a/d ratios.

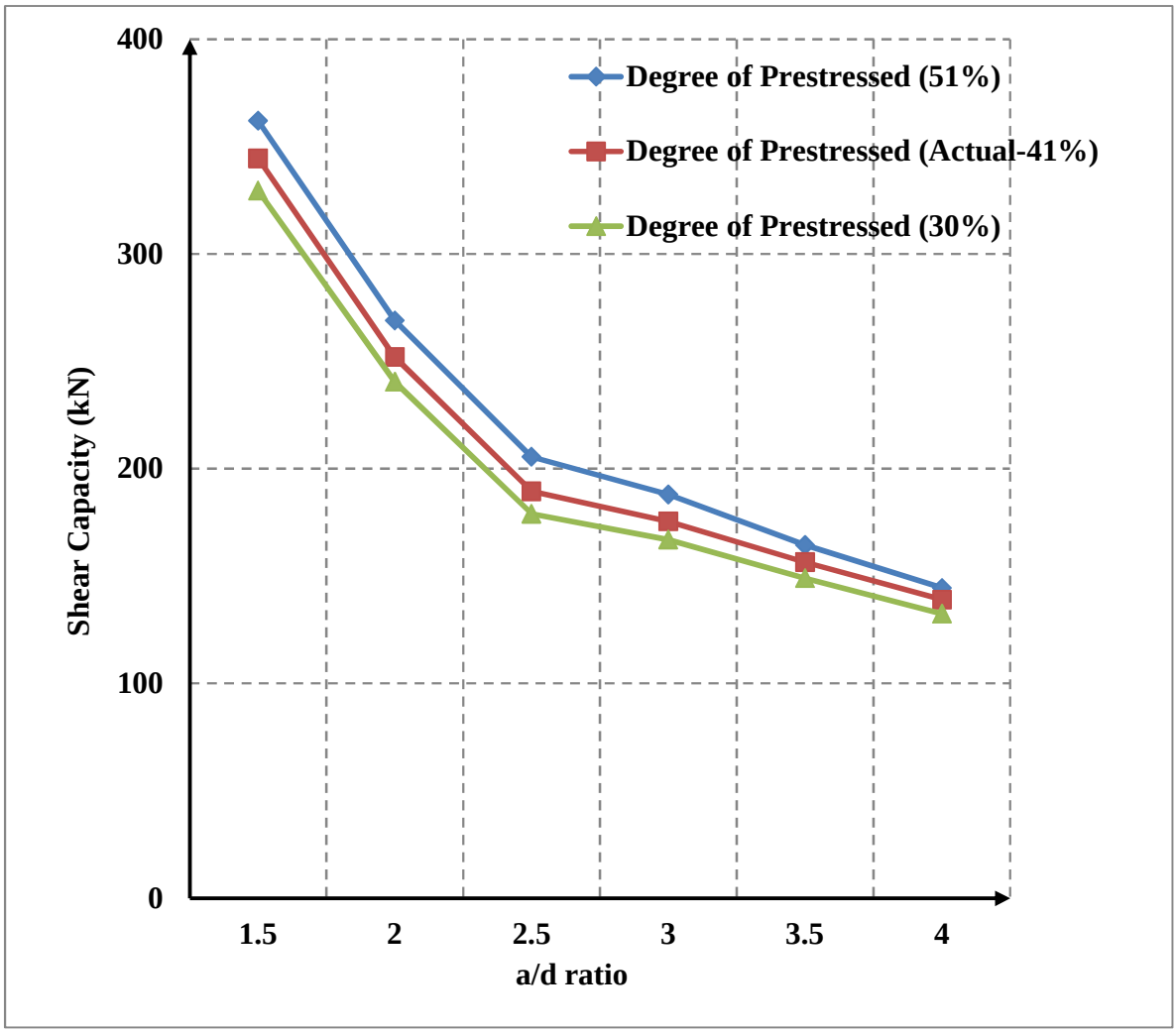

Figure (4.15): Shear Capacities Vs. a/d Ratios for Different Levels of Prestressing Force

Chapter 5

SUMMARY, CONCLUSIONS AND FUTURE WORK

5.1. Summary

The thesis investigates non-linear analysis of concrete T-beams prestressed with CFCC using FE software ANSYS. The FE models are initially constructed for the three simply-supported beams with shear span-to-depth (a/d) ratios of 1.5, 2.5 and 3.5 subjected to four-point bending and one simply-supported beam subjected to uniformly distributed load. The results of the four beams are validated against the experimental results in terms of the load-deflection response, the strain in concrete, the failure load and the mode of failure. The models are used to perform a parametric study of the beams with the a/d ratios of 2.0, 3.0 and 4.0 and with the level of prestressing forces of 30%, 41%, and 51%. For different a/d ratios, the obtained shear capacities are compared with the current shear design formulas from North American codes and guideline.

5.2. Conclusion

The findings of the present research work support the following conclusions

- The ANSYS FE models are able to analyze T-shaped concrete beams prestressed with CFCC tendons and predict the failure load and the mode of failure closely as observed in the experiments. The difference between the FEA results and experimental results are within 6% range of accuracy in terms of ultimate load prediction while the concrete strain at mid-span from the FEA is 17% lower than the test results.
- The ultimate load carrying capacities of the beams increase when the a/d ratios are decreased. The average increase in the ultimate capacities is 12% when the a/d ratios

decreased from 4.0 to 2.5. However, there are significant increases in the ultimate load carrying capacities (35%) when the a/d ratios decrease below 2.5. This is due to fact that the beams with a/d ratio less than 2.5 behave as deep beams.

- The deformability of the beams reduced noticeably when the a/d ratio is less than 2.5, while the post-cracking stiffness of the beams still increases. However, this increase in the stiffness is nominal when a/d reduces from 3.5 to 2.5.
- The average increase in the shear capacities for all the beams is 5.1% with the 37% increase in the prestressing level.
- The FE model for the beam with a/d ratio 1.5 could not accurately simulate the load-deflection response as observed in the tests. The load-deflection response obtained from the FEA is 40% stiffer than the results from the experiments in the elastic range. However, the failure load discrepancy is only 4% and the modes of failure are predicted closely by the program.
- The comparison of shear capacities from the FEA against the shear design formulas from the latest versions of CSA-S806-12, CSA-S6-10 and ACI 440-4R-04 showed that all the design codes are conservative and that the CSA-S806-12 provides similar a/d dependency of the shear as what is obtained in the analysis.
- ACI guidelines for FRP prestressed concrete beams are found to be the most conservative amongst other North American codes. The shear formula in ACI 440-4R-04 for calculating V_c for FRP prestressed concrete does not have any provisions to account for advantages of prestressing in enhancing the shear capacity of FRP prestressed concrete beams.

5.3. Future Work

Based on the findings and conclusions of the current study, the following recommendations are made for future research:

- The non-linear analysis of the prestressed beam having a/d ratio 1.5 conducted by ANSYS could not simulate the load-deflection behavior accurately so it is recommended to use other FE software such as DIANA, ABAQUAS to re-investigate such deep beams.
- The effect of different factors such as size of the beam, use of different kinds of FRP prestressing tendon and longitudinal reinforcement ratio on the shear behaviour of beams should be studied.
- It is suggested to conduct experiments on similar type of specimen using high strength concrete to investigate the effect of high strength concrete on the shear behavior. Similar numerical analysis can be performed to expand the results.
- The current North American shear design formulas are conservative in predicting the shear capacity of FRP prestressed concrete beams. Shear capacity depends on many factors but not limited to FRP material, longitudinal reinforcement ratio, prestressing level, concrete strength, geometry and span of beam. It will be useful to investigate the effect of each of these variables individually on the shear behaviour of the FRP prestressed beams to modify the current shear design formulas.

APPENDIX-A

CONCRETE STRESS-STRAIN CURVE USED IN ANSYS

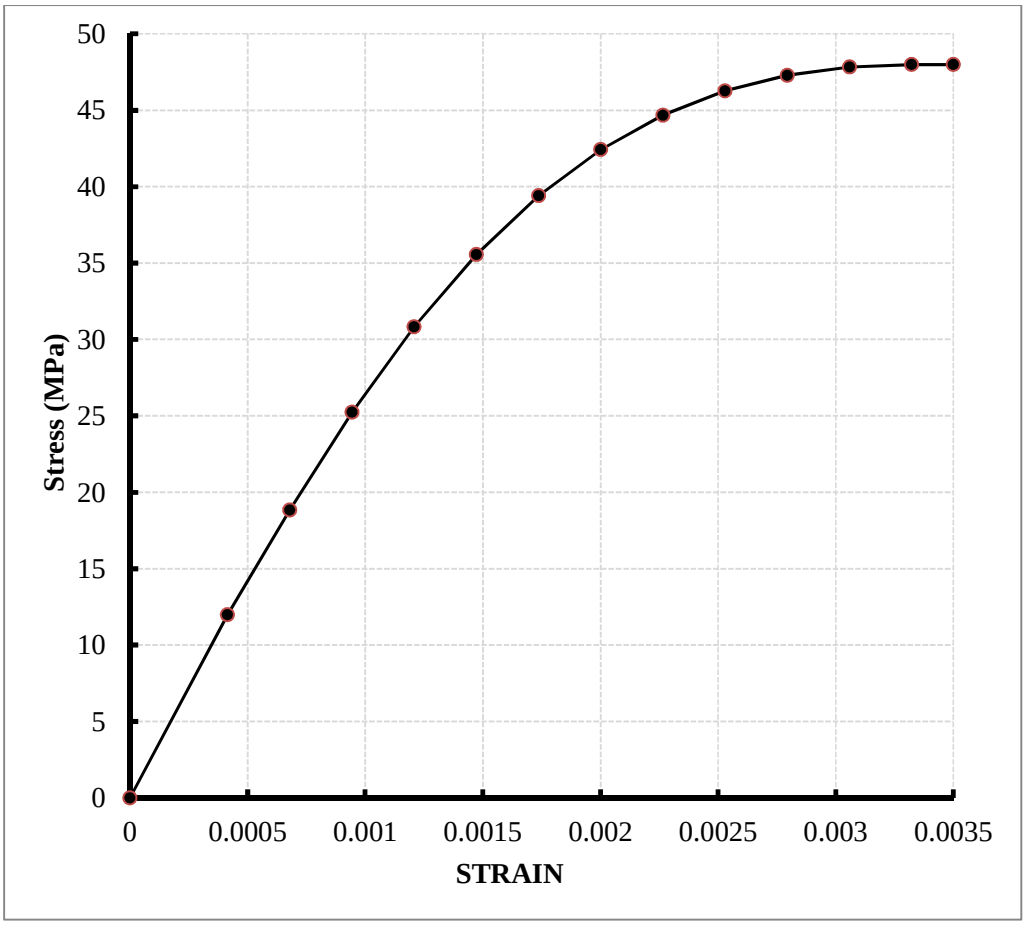

Figure (A.1): Concrete Stress-Strain Curve for the PR-3.5 Beam

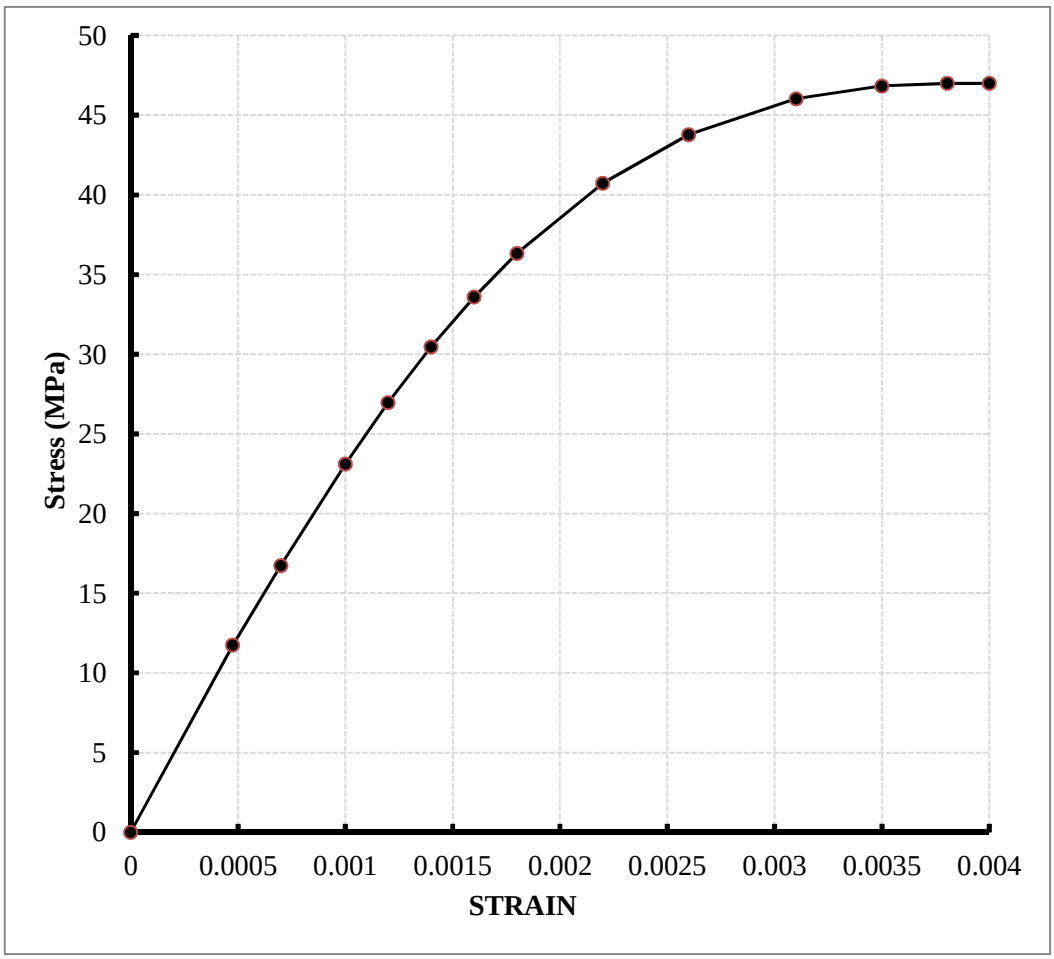

Figure (A.2): Concrete Stress-Strain Curve for the PR-2.5 Beams

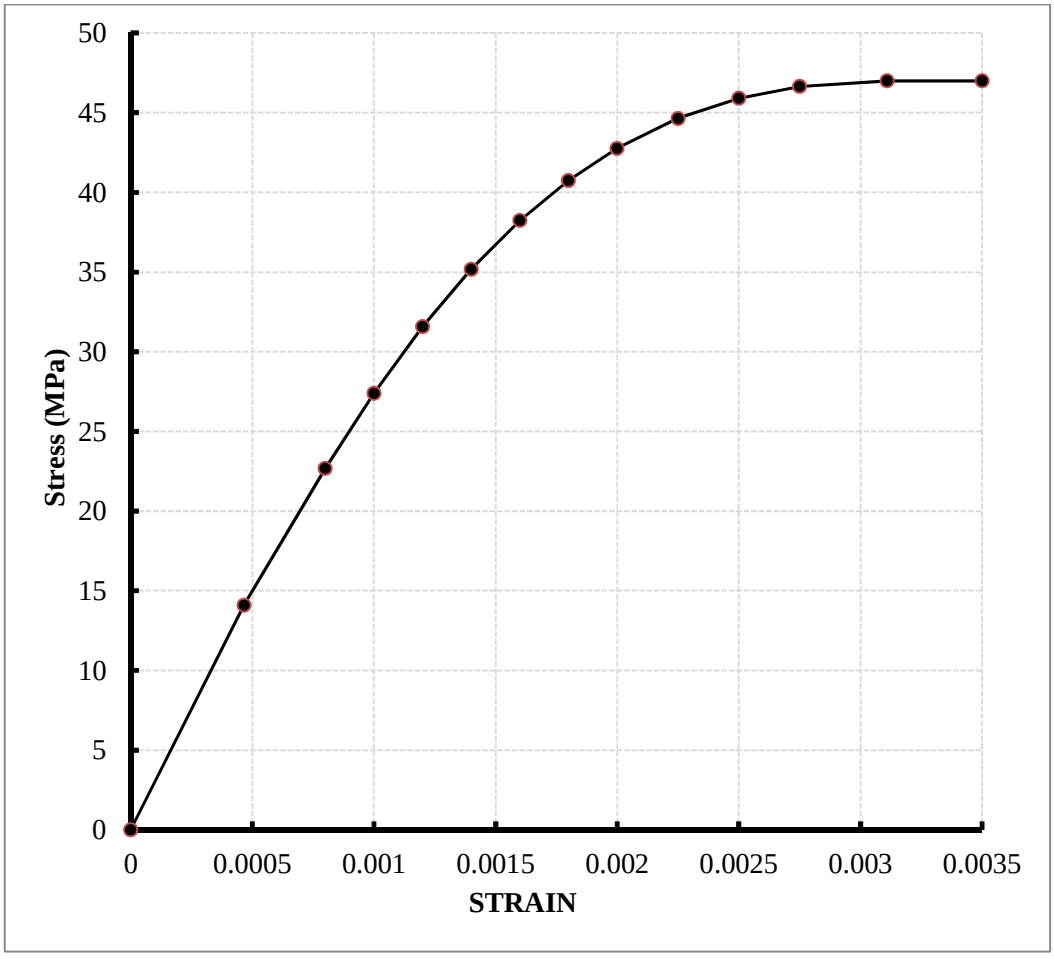

Figure (A.3): Concrete Stress-Strain Curve for the PR-1.5 Beam

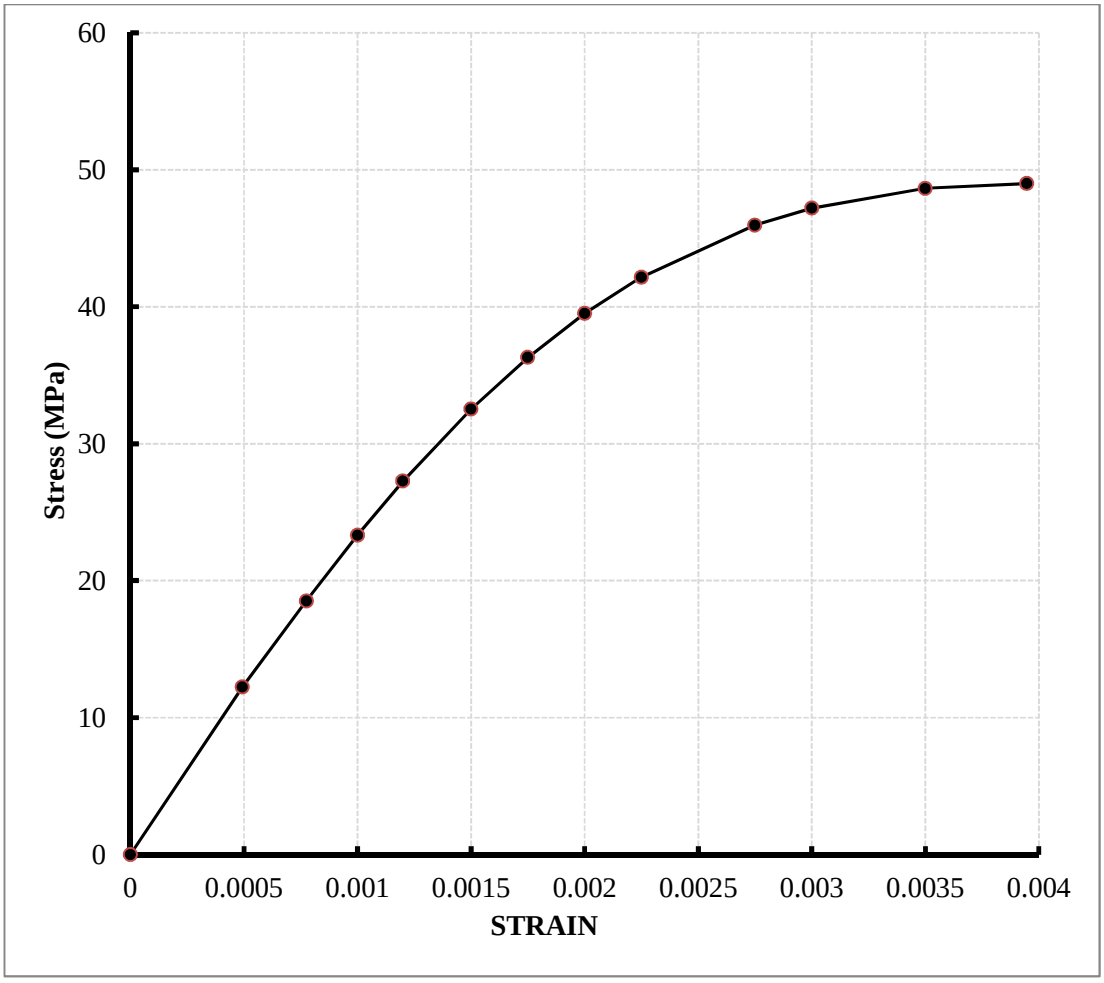

Figure (A-4): Concrete Stress-Strain Curve for the PR-U Beam

APPENDIX-B

ISOMETRIC VIEW OF THE FE MODELS

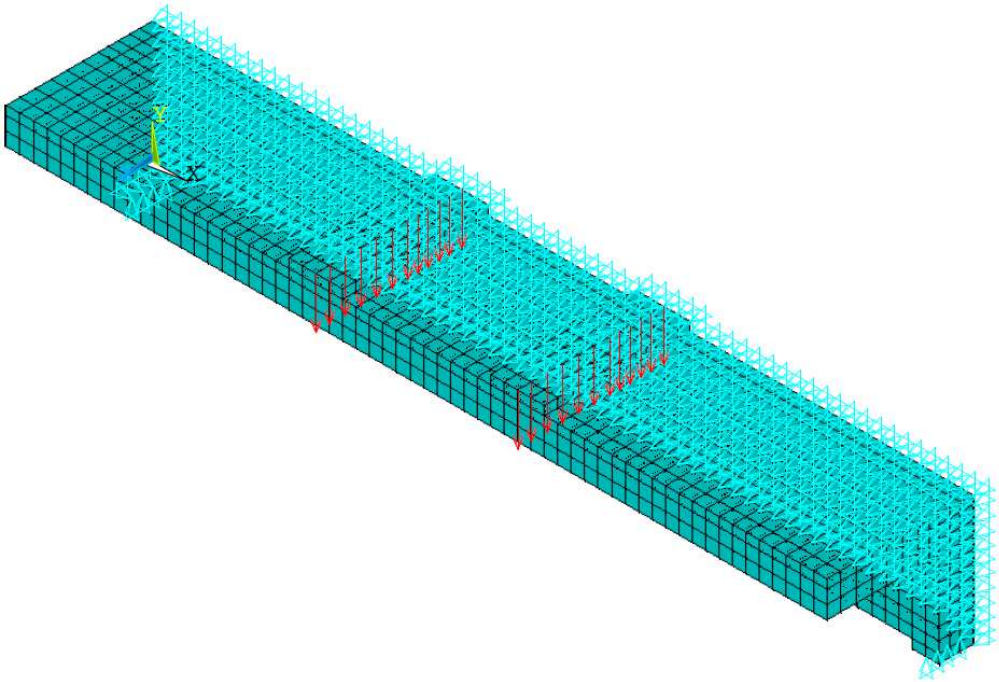

Figure (B.1): Isometric view of PR-3.5 Beam

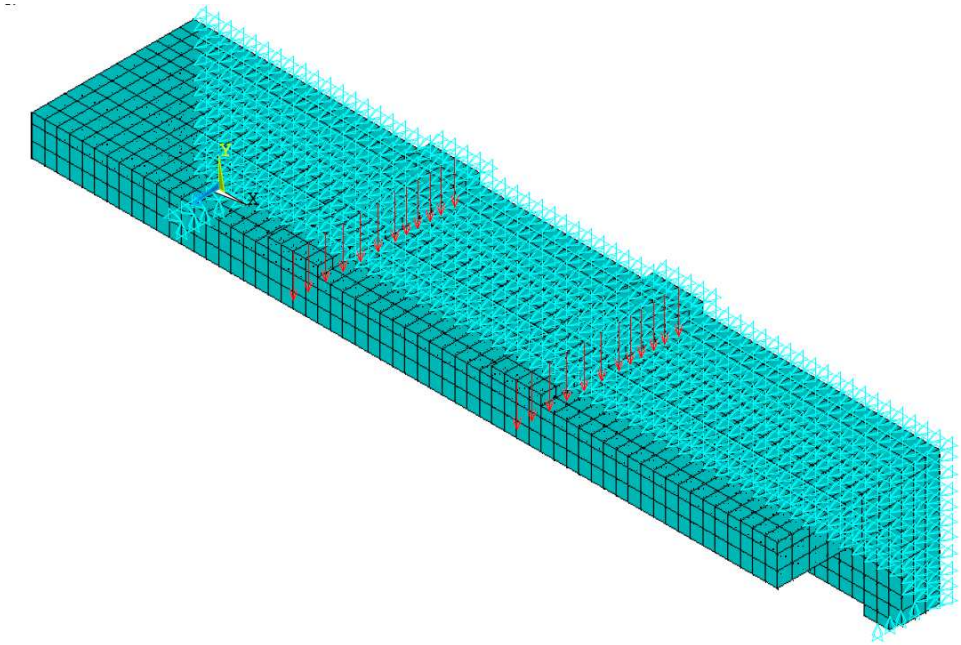

Figure (B.2): Isometric view of PR-2.5 Beam

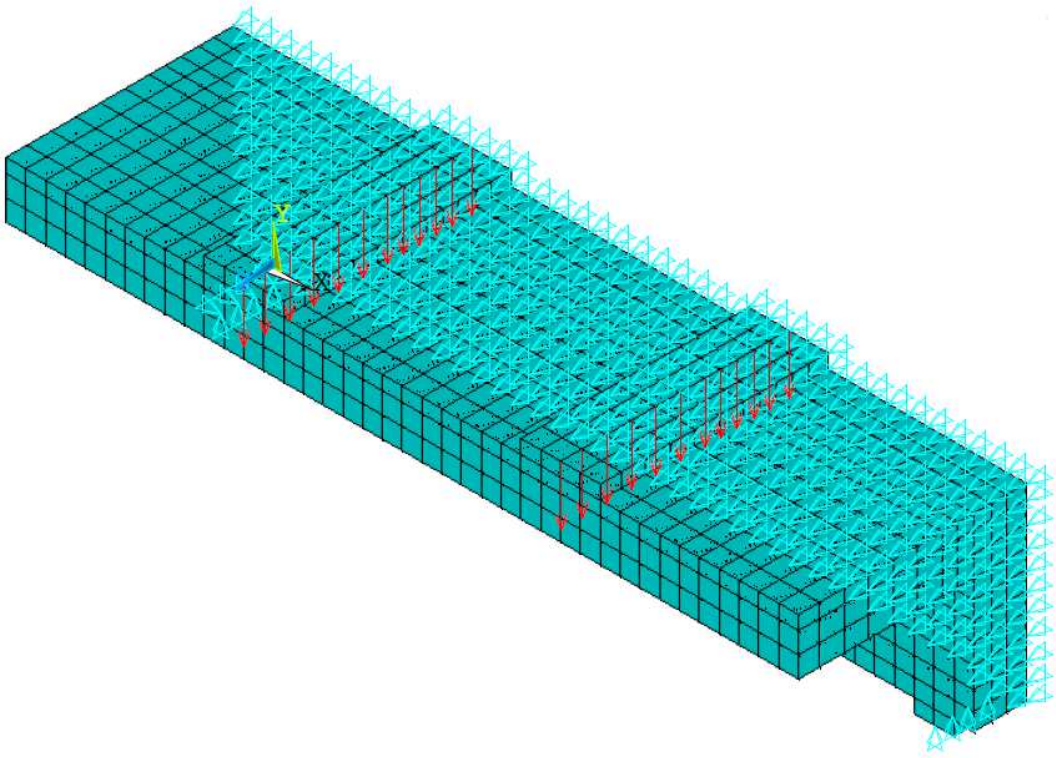

Figure (B.3): Isometric view of PR-1.5 Beam

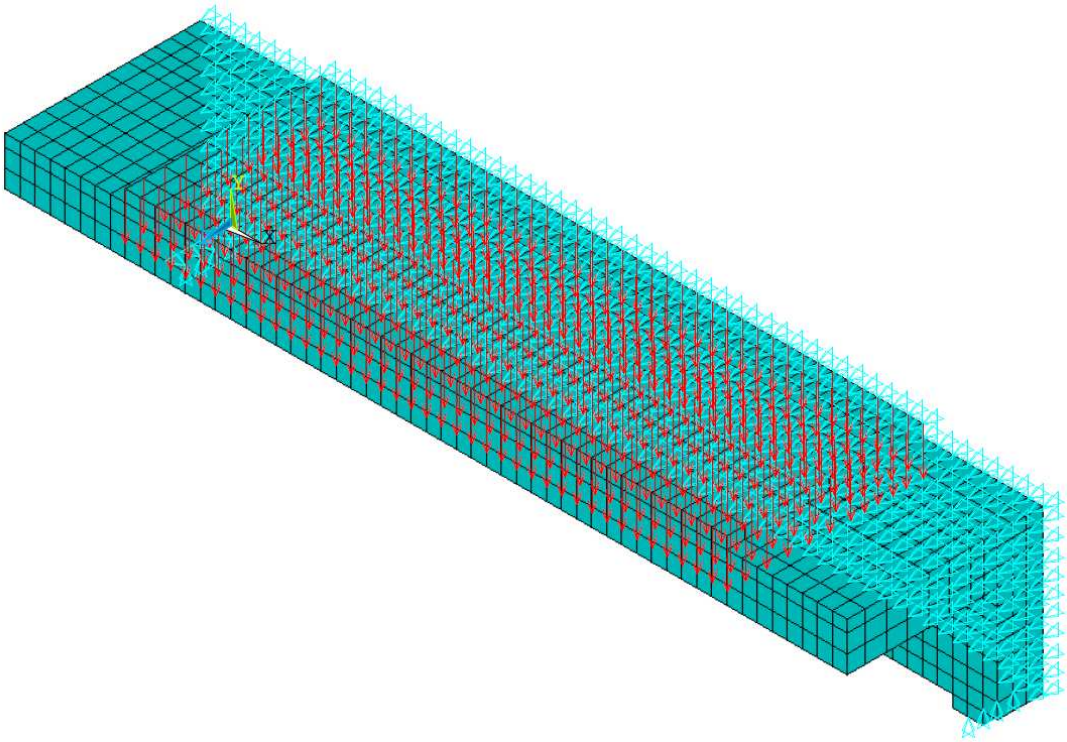

Figure (B.4): Isometric view of PR-U Beam

APPENDIX-C

SNAPS SHOWING CAMBER OF THE FE MODELS

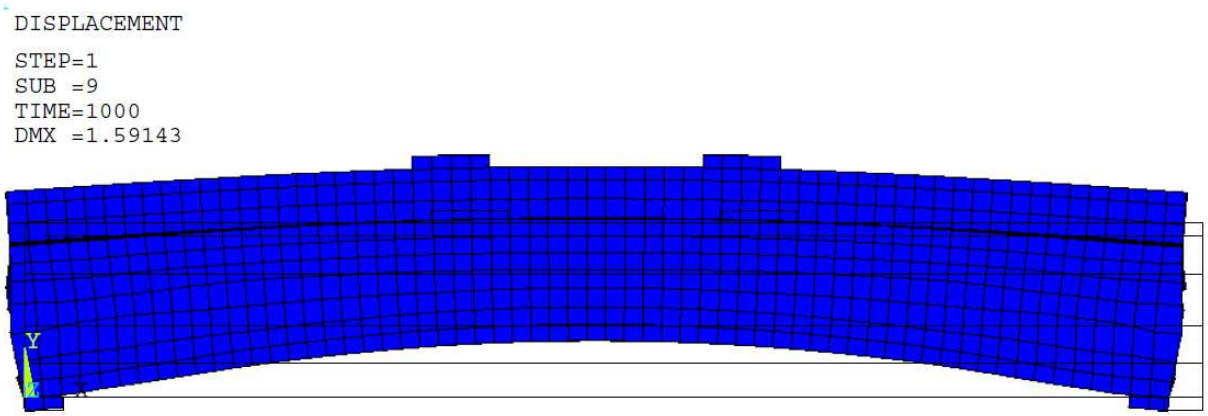

Figure (C.1): Camber of the PR-3.5 Beam

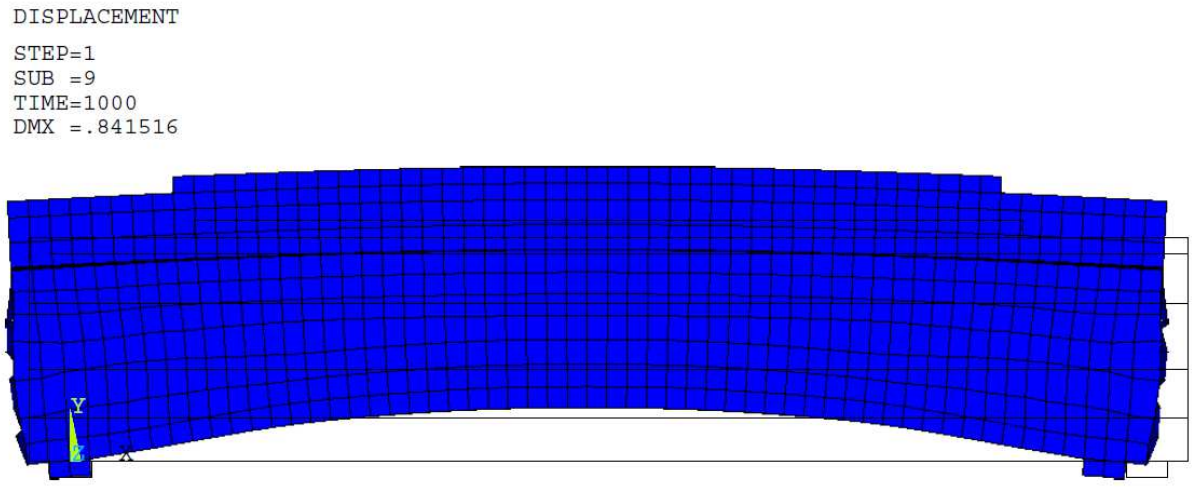

Figure (C.2): Camber of the PR-2.5 Beam

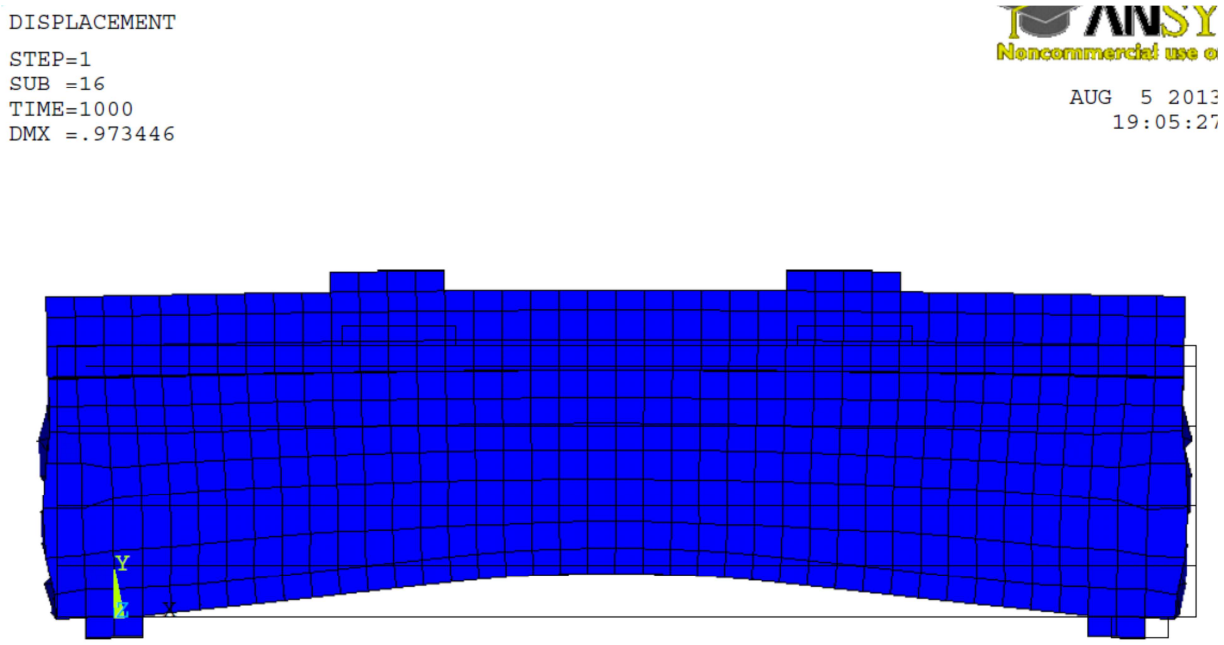

Figure (C.3): Camber of the PR-1.5 Beam

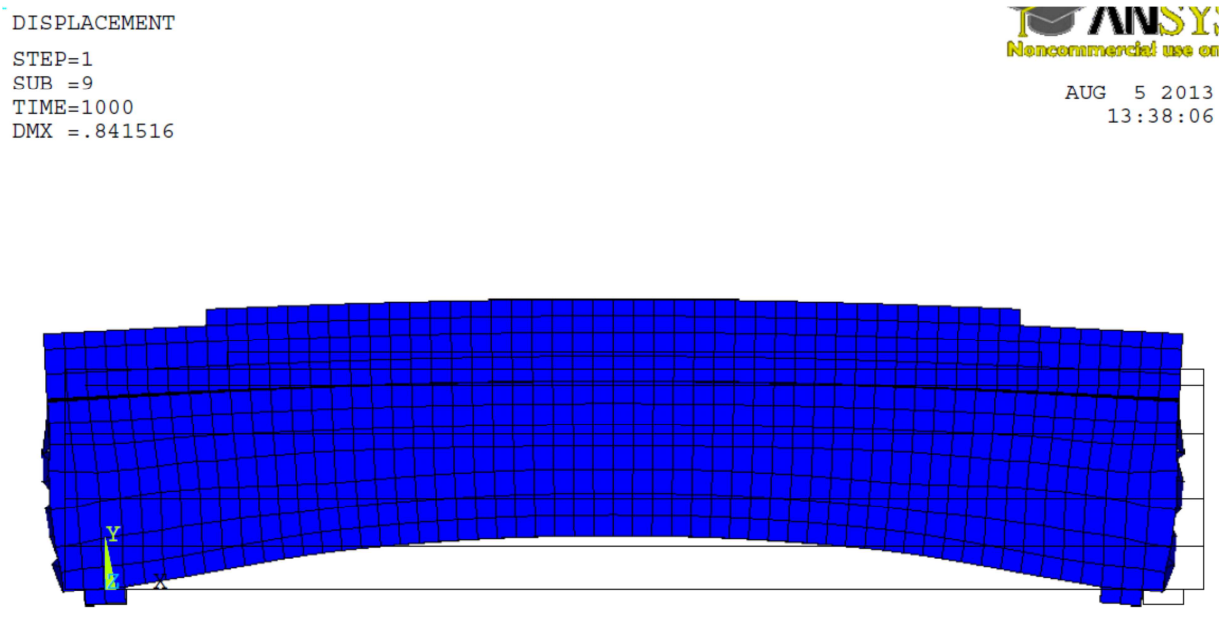

Figure (C.4): Camber of the PR-U Beam

APPENDIX-D

DEFLECTED SHAPE AT FAILURE OF THE FE MODELS

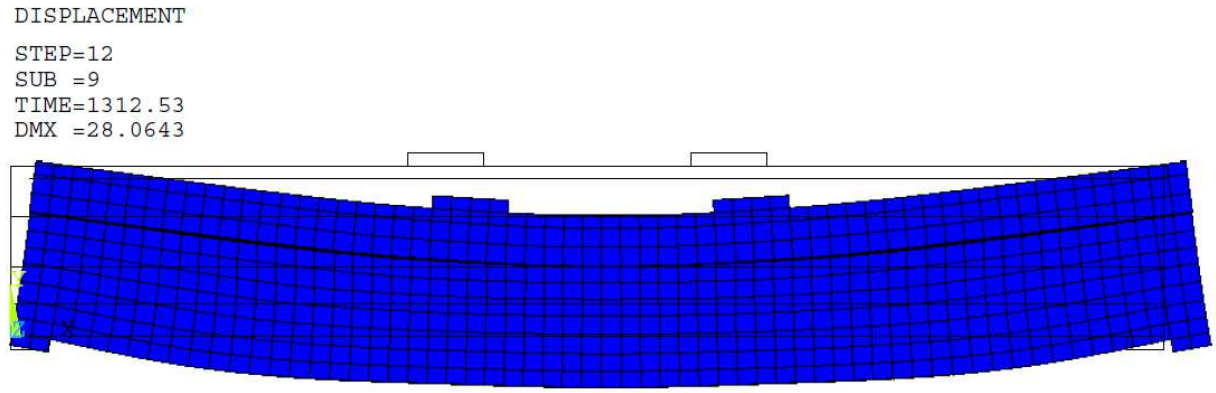

Figure (D.1): Deflected Shape at Failure for the PR-3.5 Beam

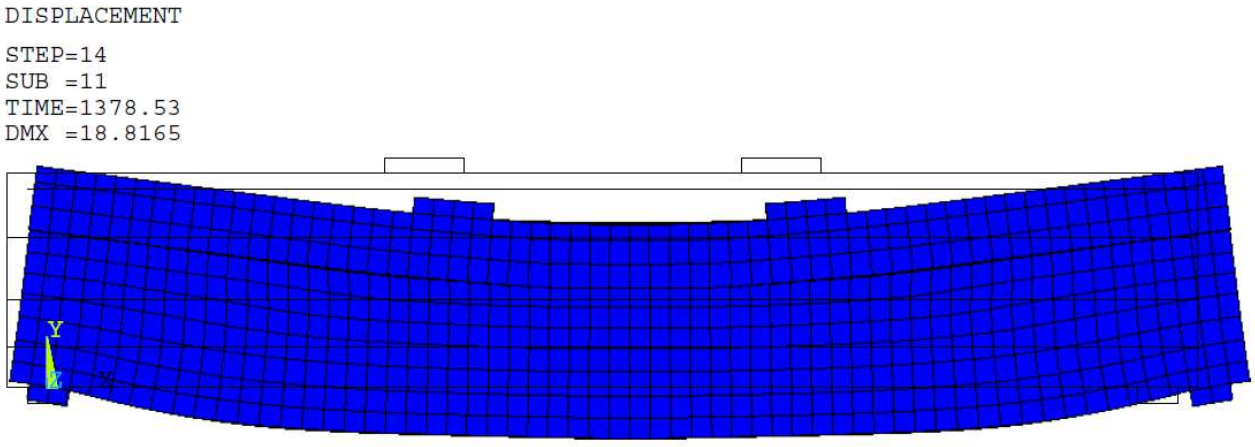

Figure (D.2): Deflected Shape at Failure for the PR-2.5 Beam

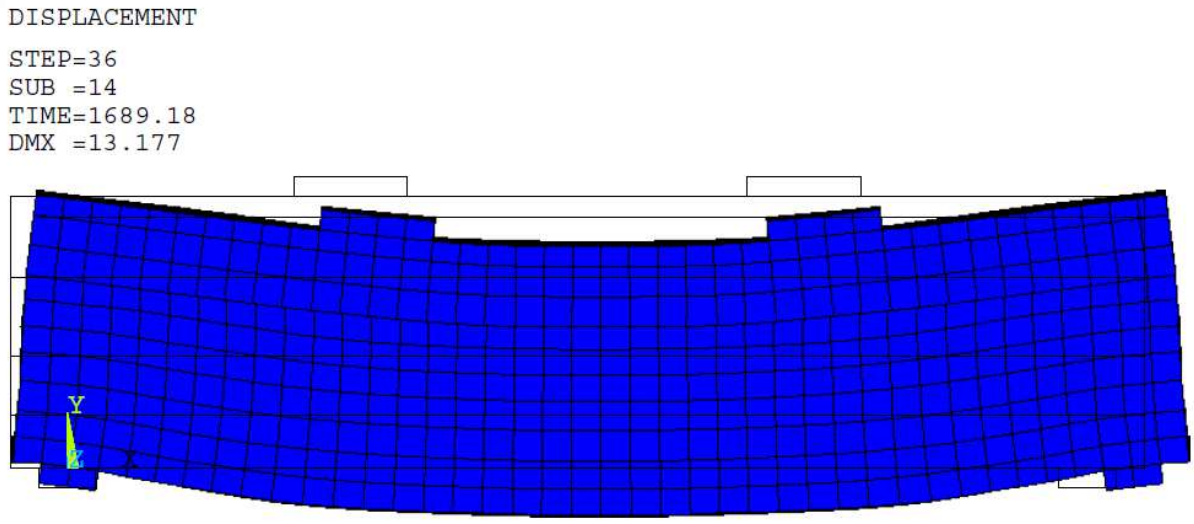

Figure (D.3): Deflected Shape at Failure for the PR-1.5 Beam

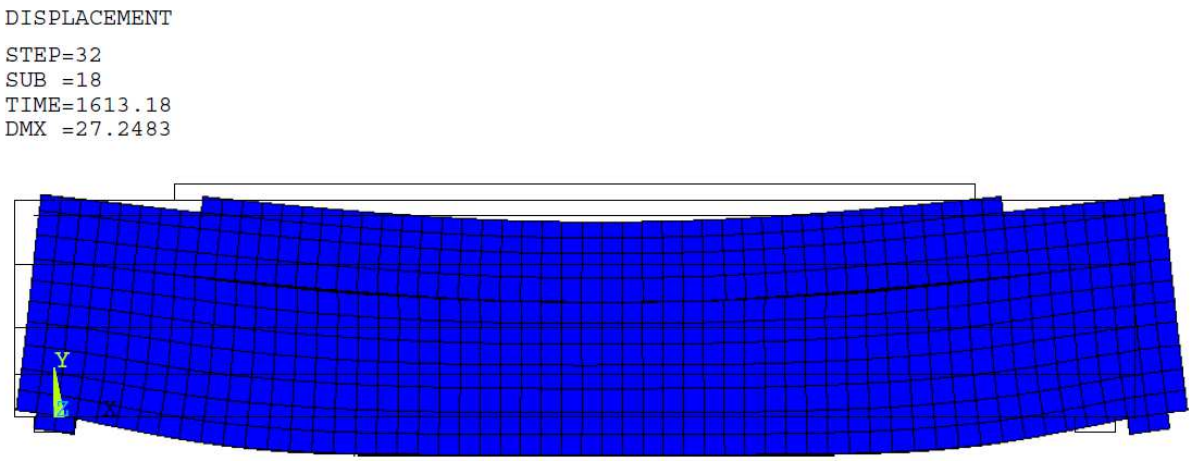

Figure (D.4): Deflected Shape at Failure for the PR-U Beam

APPENDIX-E

NORTH AMERICAN SHEAR DESIGN FORMULAS

E.1. Canadian Highway Bridge Design Code (CSA-S6-2010)

The factored shear resistance is given by (Clause 8.9.3.3)

$$V_r = V_c + V_{FRP} + \emptyset_p V_p$$

The concrete contribution to the shear strength, V_c is given by (Clause 8.9.3.4.1)

$$V_c = 2.5\emptyset_c \beta f_{cr} b d_v$$

The FRP stirrups contribution to the shear strength, V_{FRP} is given by (Clause 8.9.3.8)

$$V_{FRP} = \frac{\emptyset_{FRP} A_v \sigma_v d_v cot\theta}{s}$$

$$\sigma_v = min(\frac{[\left(0.05\frac{r}{d_s}\right) + 0.3]f_{fb}}{1.5}, E_{vFRP}\varepsilon_v)$$

E.2. Design and Construction of Building Structures with Fiber-Reinforced Polymers (CSA-S806-12)

The factored shear resistance is given by (Clause 10.10)

$$V_r = V_c + V_{FRP} + 0.5V_p + \frac{M_{dc}V_f}{M_f}$$

The concrete contribution to the shear strength, V_c is given by (Clause 8.4.4.5)

$$V_c = 0.05\emptyset_c k_m k_r f'^{1/3}_c b_w d_v$$

$$k_m = \sqrt{\frac{V_f d}{M_f}} \leq 1.0$$

$$k_r = 1 + (E_f \rho_f)^{1/3}$$

The FRP stirrups contribution to the shear strength, V_{FRP} is given by (Clause 8.4.4.9)

$$V_{FRP} = \frac{0.4\emptyset_{FRP}A_v f_{Fu} d_v cot\theta}{s}$$

$$\theta = 30 + 7000\varepsilon_x$$

$$\varepsilon_x = \frac{\frac{M_f}{d_v} + V_f + 0.5N_f - V_p - A_p f_{po}}{2(E_s A_s + E_p A_p)}$$

E.3. Prestressing Concrete Structures with FRP Tendons (ACI 440.4R-2004)

The factored shear resistance (Equation 5-1) is given by

$$\mathrm{V_r} = \mathrm{V_c} + \mathrm{V_{FRP}} + \mathrm{V_p}$$

The concrete contribution to the shear strength (Equation 5-2), V_c is given by

$$V_c = 0.17\sqrt{f'_c} b_w d_v$$

The FRP stirrups contribution to the shear strength (Equation 5-3), V_{FRP} is given by

$$V_{FRP} = \frac{A_v f_{fb} d_v}{s}$$

$$f_{fb} = \min(\emptyset_{bend} f_{Fu}, 0.002E_{vFRP})$$

$$\emptyset_{bend} = (0.11 + 0.05\frac{r}{d_s})$$

The beams with a/d ratios less than 2.5 act as a deep beam so the shear formulas mentioned above are not valid for the beams with a/d ratios 1.5 and 2.0. The procedures outlined for CSA and ACI methods in the CPCI design handbook are followed to estimate the shear capacities (CPCI Handbook 2007).

[1] American Concrete Institute (ACI), A. C. (2005). 318-05: *Building Code Requirements for Structural Concrete and Commentary.* Farmington Hills, Michigan: American Concrete Institute.

[2] (ACI), A. C. (2006). *ACI Committee 440 Report (ACI-440.1R-06): Guide for the Design and Construction of Structural Concrete Reinforced with FRP Bars.* Farmington Hills, Michigan, USA: American Concrete Institute.

[3] (ACI), A. C. (2004). *ACI Committee 440 Report-ACI 440-4R-04: Prestressing Concrete Structures with FRP Tendons.* Farmington Hills, Michigan, USA: American Concrete Institute.

[4] ASCE-ACI Committee 426 Report. (June 1973). "*The Shear Strength of Reinforced Concrete Members*" Journal of Structural Division: American Concrete Institute.

[5] Association, C. S. (2010). *CAN/CSA-S6-10-Canadian Highway Bridge Design Code.* Mississauga, Ontario: Canadian Standards Association.

[6] ANSYS (2013) ANSYS Release 14.0 Finite Element Analysis System, SAS IP, Inc.

[7] Ananth Ramaswamy, Job Thomas (2006). "*Nonlinear Analysis of Shear Dominant Prestressed Concrete Beams using ANSYS*," ACI Structural Journal, 103(3), 427-435.

[8] A. Kasat, V.Varghese (2012). "*FEA of Prestressed Concrete Beams*," International Journal of Advance Technology in Civil Engineering, Vol.1, Issue.3, ISSN-2231-5721

[9] B.R.Niranjan, S.S.Patil (2012). "*Analysis of RC Deep Beams by FEM*," International Journal of Modern Engineering Research (IJMER), Vol2, Issue.6, ISSN-2249-6645

[10] (CSA), C. S. (2004). *CAN/CSA-A23.3-04- Design of Concrete Structures.* Toronto, Ontario: Canadian Standards Association.

[11] (CSA), C. S. (2012). *CAN/CSA-S806-12- Design and Construction of Building Structures with Fibre-Reinforced Polymers.* Canadian Standards Association.

[12] Canadian Precast/ Prestressed Concrete Institute. (2007). *Design Manual Precast and Prestressed Concrete.* Ottawa, Ontario: Canadian Precast/ Prestressed Concrete Institute.

[13] Collins, M. P., & Mitchell, D. (1997). *Prestressed Concrete Structures.* Ontario: Response Publications.

[14] E.Cosenza, G.Manfredi and R.Realfonzo (1995). "*Analytical Modeling of Bond between FRP Reinforcing Bars and Concrete*" ASCE-Journal of Composites for Construction, ISSN-5621-2765

[15] El-Hacha, R. (2005). Prestressing Concrete Structures with FRP Tendons (ACI 440.4R-04). *Structures Congress 2005: Metropolis and Beyond*, (pp. 1-8). New York.

[16] F.Leonhardt, R.Walter (1961). "*The Stuttgart Shear Tests,*" Cement and Concrete Association, Vol.56, No.12 (1961), London.

[17] Farid H Abed, Abdullah Al-Rahmani, Ahmed H.Al-Rahmani (2013). "*Finite Element Simulation of the Shear Capacity of GRRP Reinforced Concrete Short Beams,*" Institute of Electrical and Electronic Engineer (IEEE), New York.

[18] I.Safiullah, M.A.Hossain, M.A.Amin (2011). "*Nonlinear Analysis of RC Beam for Different Shear Reinforcement Patterns by FEA,*" International Journal of Civil and Environmental Engineering IJCEE-IJENS Vol.11, No.1

[19] Hayder H.H.Kamonna (2010). "*Nonlinear Analysis of Steel Fiber Reinforced Concrete Beams by ANSYS,*" KUFA Journal of Engineering ISSN 2071-5528, VOL 2, Number 1, pp.109-124.

[20] Kachlakev, D., Miller, T., Yim, S., Chansawat, K. and Potisuk, T. (2001). "*Finite Element Modeling of Reinforced Concrete Structures strengthened with FRP Laminates.*" Final Report SPR-316, Oregon Department of Transportation, Salem, Oregon.

[21] Mady, M. H. A. (2011). "*Seismic Behaviour of Exterior Beam-Column Joints Reinforced with FRP bars and Stirrups*," Ph.D. Thesis, Department of Civil Engineering, University of Manitoba, Winnipeg, Manitoba.

[22] Mostafa, A.T.El-Mogy (2011). "*Behavior of Continuous Concrete Beams Reinforced with FRP Bars*," Ph.D. Thesis, Department of Civil Engineering, University of Manitoba, Winnipeg, Manitoba.

[23] MacGregor, J. G., & Bartlett, F. (2000). *Reinforced Concrete Mechanics and Design.* Scarborough, Ontario: Prentice-Hall Canada Inc.

[24] P.Paramasivam, Kiang-Hwee Tan, K.Murugappant (1995). "*FEA of Partially Prestressed Steel Fiber Concrete Beams in Shear*," Elsevier Science Inc. New York, ISSN 1065-7355

[25] Precast/Prestressed Concrete Institute (PCI). (2007). "*Design Handbook*," 6th Edition, Precast/Prestressed Concrete Institute, Chicago, IL.

[26] Mirpayam Nabipaylashgari (2012). "*Shear Strength of Concrete Beams Prestressed with CFRP Cables*," Master's Thesis, Department of Civil Engineering, University of Manitoba, Winnipeg, Manitoba.

[27] M.R.Salamy, H.Kobayashi and Sh.Unjoy (2005). "*Experimental and Analytical Study on RC Deep Beams*," Asian Journal of Civil Engineering Vol6, No.5

[28] Mahamut Sami Celal (2011). "*Shear Behavior of Precast/Prestressed Hollow-Core Slab*," Master's Thesis, Department of Civil Engineering, University of Manitoba, Winnipeg, Manitoba.

[29] Nabil Grace, M.ASCE, Kenichi Ushijima, Prince Baah and Mena Bebawy (2013). "*Flexural Behavior of a Carbon Fiber–Reinforced Polymer Prestressed Decked Bulb T-Beam Bridge System*" ASCE, ISSN-1943-5614

[30] Samir M.O.H.Dirar and Chris T.Morley (2005). "*Nonlinear Finite Element Analysis of Reinforced Concrete Deep Beams*," VIII International Conference on Computing Plasticity, Barcelona

[31] Sudheer Reddy, R.Rao and G.Rao T.D (2011). "*Evaluation of Shear Resistance of High Strength Concrete Beams without Web Reinforcement using ANSYS*," APRN Journal of Engineering and Applied Sciences Vol6, No.2, ISSN-1819-6608

[32] Tavarez, F.A., (2001), "*Simulation of Behavior of Composite Grid Reinforced Concrete Beams Using Explicit Finite Element Methods*," Master's Thesis, University of Wisconsin-Madison, Madison, Wisconsin

[33] T.H. Kim, J.H. Cheon, H.M.Shin (2011). "*Evaluation of Behavior and Strength of Prestressed Concrete Deep Beams using Nonlinear Analysis*," Journal of Concrete and Computers, Vol.9, No.1 (2012) 63-79, Korea.

[34] Willam, K.J. and Warnke, E.P. (1974), "*Constitutive Model for Triaxial Behaviour of Concrete*," Seminar on Concrete Structures Subjected to Triaxial Stresses, International Association of Bridge and Structural Engineering Conference, Bergamo, Italy, 174.

[35] Wolanski, A. J. (2004). "*Flexural Behavior of Reinforced and Prestressed Concrete Beams using Finite Element Analysis*," M.Sc. Thesis, Marquette University, Milwaukee, Wisconsin

[36] Y.J.Kim (2010). "*Modeling of Concrete Beams Prestressed with AFRP Tendons*," Challenges, Opportunities and Solutions in Structural Engineering and Construction-Taylor and Francis Group, London, ISBN 978-0-415-56809-8

[37] Zuohu Wang and Xiuli Du (2011). "*Nonlinear Linear Analysis of Concrete Beams Prestressed with FRP Tendons*," Mechanic Automation and Control Engineering (MACE), 2011 Second International Conference.